VILNIUS GEDIMINAS TECHNICAL UNIVERSITY

ANTANAS GUSTAITIS' AVIATION INSTITUTE

DEPARTMENT OF AERONAUTICAL ENGINEERING

Mustafa Etem Surucu

An Analysis of Integrated Vehicle Health Management Systems in Unmanned Aerial Vehicles and Autonomous Aircrafts

Master's degree Thesis

Study programme AEROSPACE ENGINEERING,

Code 6211EX060

Vilnius, 2023

VILNIUS GEDIMINAS TECHNICAL UNIVERSITY

ANTANAS GUSTAITIS AVIATION INSTITUTE

DEPARTMENT OF AERONAUTICAL ENGINEERING

APPROVED BY

Head of Department

_____

(Signature)

Darius Rudinskas
(Name, Surname)

_____

(Date)

Mustafa Etem Surucu

An Analysis of Integrated Vehicle Health Management Systems in Unmanned Aerial Vehicles and Autonomous Aircrafts

Master‘s degree Thesis

Study programme AEROSPACE ENGINEERING,

Code 6211EX060

Supervisor: (Title, Name, Surname) (Signature) (Date)

Table of Contents

Table of Figures

Introduction

IVHM system can avoid unnecessary cost increases due to the realization of additional functions. First, the FMECA of the USV is carried out from the equipment layer to the system layer according to the system structure of the USV. This aims to identify key equipment significantly affecting navigation safety or mission success of the USV. Then, the key equipment of the USV and overall functional requirements of the USV on the IVHM system are analyzed based on use and maintenance requirements (HU J & CAI W T., 2021).

Unmanned aerial vehicles and autonomous aircraft have emerged as integral components of modern aviation systems, offering a wide range of applications in various domains such as surveillance, reconnaissance, cargo transportation, and remote sensing. Ensuring the reliable and efficient operation of these vehicles is of utmost importance to guarantee the safety of operations and optimize their performance. IVHM systems have emerged as a critical approach to monitor and manage the health and performance of UAVs and autonomous aircraft in real-time.

The analysis of sensor data plays a crucial role in IVHM systems, providing valuable insights into the health status and behavior of the vehicles. Among the various sensors employed in UAVs and autonomous aircraft, the accelerometer and gyroscope sensors are particularly important for capturing and measuring the vehicles' motion and orientation.

This research endeavors to delve into the logs obtained from the accelerometer and gyroscope sensors which form part of flight log obtained from university. Our primary objective is aimed at exploring IVHM systems used within these sensors by examining the data provided via flight log. Through detailed scrutiny of accelerometer readings we can extract critical information regarding linear acceleration exhibited by UAVs while being able to identify any motion patterns that may be anomalous or deviate from expected behavior patterns. Similarly analyzing gyroscope outputs enables us to investigate rotational movements being made by UAVs while also uncovering irregularities or disturbances that might hinder their performance negatively.

To fulfill our objectives we employ advanced techniques including statistical analysis, signal processing algorithms along with effective visualization methods which aid us in exploring various key attributes within accelerometer & gyroscope sensor readings. These

insights provide a comprehensive understanding of UAVs' & autonomous aircrafts' performance levels dependability quotient as well as overall health status.

This analysis intends to expand our understanding of IVHM systems concerning UAVs and automated planes. By detecting possible issues or abnormalities within accelerometer and gyroscope sensor data, this research seeks to support proactive maintenance tactics as well as facilitate timely interventions for assured safe operation and improved effectiveness of such aeronautical units.

Ultimately, this scrutiny into IVHM linked to accelerometer and gyroscope-based monitoring can aid advancements within UAVs' realm by offering valuable insights that enable optimal vehicle health checkup strategies.

1. Literature Review

The literature review chapter provides a comprehensive analysis of the existing research and knowledge in the field of UAVs, IVHM systems, and sensor technologies. This chapter aims to synthesize and summarize relevant literature, exploring the diverse applications and characteristics of UAVs, sensor technologies, and their integration within the aerospace domain. By reviewing and analyzing key studies, this chapter establishes a foundation of knowledge to inform the subsequent research and development efforts in the field.

1.1 Unmanned Aerial Vehicles

Different types of Unmanned Aerial Vehicles (UAVs) with distinctive characteristics, such as supported altitude, speed, and energy autonomy, are suitable for different applications. Generally, UAVs are classified according to their supported altitudes into Low-Altitude Platforms (LAP) and High-Altitude Platforms (Al-Hourani et al., 2014). Furthermore, UAVs can be classified into rotary-wing and fixed-wing. The former are appropriate for cases that require UAVs that can remain at steady positions, whereas the latter are suitable for applications that demand UAVs travelling at high speeds and covering large distances (Zeng et al., 2016). In an IoT environment, due to the limited energy capacity of the participating devices, suitable LAP UAVs of the rotary-wing type can be efficiently and dynamically positioned to allow Internet of Things (IoT) devices to transmit with minimum power. A related framework towards this direction is introduced in Reference (Mozaffari et al., 2017), while authors in Reference (Soorki et al., 2016) introduce a resource-allocation scheme for improving energy consumption at cluster heads that use aerial base stations. (Lagkas et al., 2018). UAVs have found many applications, such as condition monitoring, geographical mapping, and performing certain dangerous tasks, wherein the sensor technologies are indispensable for achieving these functions (van Blyenburgh, 1999)–(Zhu & Pong, 2019). These sensors include accelerometers, tilt sensors, engine intake flow sensors, magnetic sensors (electronic compasses), and current sensors (Winkler, 2016). Among these sensors, current sensors play an important role for a healthy operation of UAVs such as to prevent overcharging and safeguard against overcurrent, (Daponte et al., 2017).

The UAVs undergo various power profiles in different parts of the UAV mission, such as takeoff, hovering, and landing. The accuracy of current sensing is critical, as they undertake the following tasks (see Fig. 1). The overcharging condition should be totally avoided because

it can generate the heat and gases in batteries, resulting in the irreversible damage (Miguel Rasgado Baião et al., 2017). Second, the current sensors can measure the energy consumption of batteries for determining the remaining flight time (Jin et al., 2003). In UAVs, the flight time is critically dependent on the battery life. A “dead stick” condition in which the battery becomes completely drained during flight can be disastrous (Unmanned Systems Technology, 2017). Finally, the real-time current measured by current sensors can be used by the protection system to alert when there is a system fault (Saha et al., 2011).

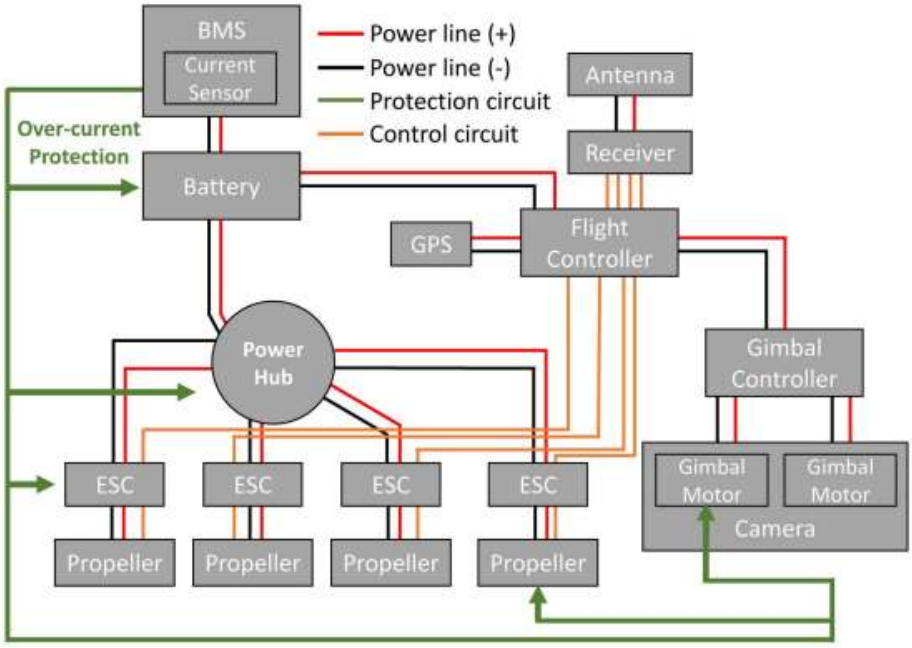

Fig. 1. Circuitry of a UAV, including the battery management system (BMS), current sensor, battery, power hub, electronic speed controller (ESC), propeller, and so on (van Blyenburgh, 1999).

1.2 Health Management Systems

Integrated System Health Management (ISHM) systems are primarily responsible for diagnostic and prognostic functions across a wide array of aerospace, defence and transport systems to enhance decision-making and provide opportune assessments regarding a system’s state-of-health and availability to operations and maintenance crew (Jennions, 2013). The National Aeronautics and Space Administration (NASA) introduced Vehicle Health Monitoring (VHM) which expanded this concept to include appropriate sensors and software to monitor multiple aspects of aerospace vehicles (Woodard, S. E.,2003).

However, there is not only one definition of Integrated Vehicle Health Management (IVHM). For instance, according to NASA; safety and reliability improvement, cost reduction, mission enhancement, and the enabling of new capabilities and missions (NASA, 1992).

By providing integrated health monitoring and supporting Condition-based Maintenance (CBM), IVHM aims to minimize Maintenance Repair and Overhaul (MRO) costs and enhance aircraft availability in the aviation sector (Ezhilarasu et al., 2019). In terms of the history, the growth of aircraft design and operations eventually contributed to the continually updated maintenance programs.

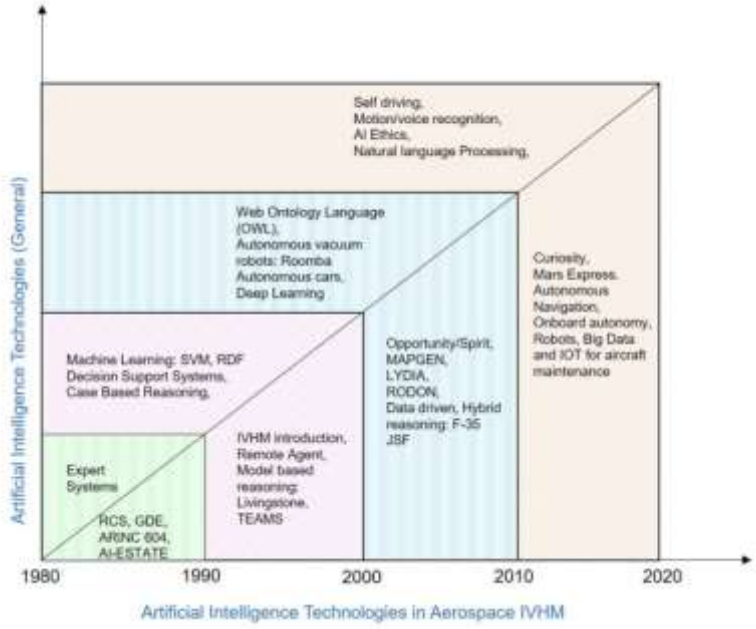

Fig. 2. Trend of AI technologies in Aerospace IVHM versus general AI technologies (Ezhilarasu et al., 2019).

When technology moved toward digital systems in the 1980s (Fig. 2), built-in test (BIT) circuits were tested electronically to detect faulty Line Replaceable Units (LRU). This replaced the earlier method of troubleshooting, which involved testing the circuit for continuity in mechanical and analog aircraft systems (Johnson et al., 2011). For B747 aircraft, Centralized Maintenance Computers (CMC) were created in the early 1990s to assess the condition of numerous LRUs (Ezhilarasu et al., 2019).

Modular systems, data-driven approaches to diagnosis, and loadable databases were all features of early 2000s maintenance systems like Honeywell Prime Epic Aircraft Diagnostic Maintenance Systems (ADMS) (Johnson et al., 2011).

The IVHM sector is utilizing big data analysis and cloud-based computing in the current decade to improve real-time health monitoring. Additionally, the aerospace sector, that includes Rolls Royce, is exploring the use of robotics to examine systems and determine whether maintenance is necessary (CNBC, 2018).

In recent years, with evolution of the new paradigm of IVHM encompassing all or several of the aircraft systems, Structure health Management (SHM) is becoming a part of the IVHM strategy and issues alerts. These alerts serve as early warnings or notifications to take suitable actions "in-advance", thereby ensuring mission readiness and safety rapidly and economically (Mangalgiri & Harinarayana, 2017).

Regarding the subsystems of IVHM, two subsystems set up the IVHM: the diagnostic subsystem and the prognostic subsystem Williams (2006). To better understand IVHM subsystem Prajapati et al. (2018) defined the term 'diagnostic subsystem'; it is responsible for fault detection, regardless of whether fault has actually occurred, and in the event of a fault, it identifies the cause of the fault, thus establishing the association between fault diagnosis, detection, isolation, and cause determination, while the prognostic subsystem is employed to estimate the remaining useful life (RUL) of the intricate critical system, encompassing its subsystems and components. In terms of the second subsystem, namely the prognostic subsystem, its purpose is to facilitate real-time assessment, continuous monitoring of operational health, and estimation of the remaining useful life for both complex systems and their individual components (Prajapati et al., 2018).

Health data are collected from vehicle components, structures, and elements and used to make diagnoses and prognoses of the present and future health of the vehicle. This information is further processed to formulate appropriate operation and support actions and presented to the people who should decide and execute the actions. Here, the first critical issue is that information regarding vehicle condition must be acted upon to generate reactive plans rather than merely processing health data and presenting them for later manipulation and use (Benedettini et al., 2009).

IVHM is the unified capability of systems to assess the current or future state of the system health and integrate that picture of system health within a framework of available resources and operational demand. Prognostic and Health Management (PHM) can be defined as the ability of assessing the health state, predicting impending failures and forecasting the expected RUL of a component or system based on a set of measurements collected from the

aircraft systems (Vachtsevanos et al., 2006). It comprises a set of techniques, which use analysis of measurements to assess the health condition and predict impending failures of monitored equipment or system (Paixão de Medeiros et al., 2014).

Developments in Prognostics and Health Monitoring (PHM) technology within the aeronautical sector have been of value for aircraft operators, MRO (Maintenance, Repair and Overhaul) service providers, aircraft manufacturers and OEMs (Original Equipment Manufacturers) to achieve important competitive advantages such as reduction in operational cost and increase in fleet reliability (Rodrigues & Yoneyama, 2012; Paixão de Medeiros et al., 2014).

Moving on now to consider the benefits of IVHM. In his work, Williams (2006) discusses the benefits of employing an IVHM system in fleet management, particularly in terms of allocating alternative tasks based on variations in component capabilities and conditions within the vehicle. Furthermore, the author highlights the role of IVHM in facilitating an efficient vehicle turnaround process. From a maintenance perspective, an IVHM system plays a significant role by diminishing the need for frequent inspections, minimizing uncertainties surrounding faults, reducing repair time, and mitigating the unnecessary removal of potentially viable components (Prajapati et al., 2018). From another perspective, according to Hess and Fila (2002) an IVHM expands inspection coverage and offers early notice of maintenance needs and the implementation of an IVHM system enables more proactive management and enhances responsiveness by providing timely access to malfunction alerts. This allows for effective actions to be taken promptly in response to requirements and support operations (Hess et al., 2004). Similarly, in order to enhance the reliability of the supply chain, it is imperative to consistently update data regarding part utilization and resource allocation within the logistics sector (Hess & Fila, 2002).

1.3 Sensor Review

This chapter focuses on evaluating sensors and their significance within IVHM systems. It examines the role of sensors in enhancing connectivity, low latency, and reliable communication for drones as smart devices within the Internet of Things (IoT) framework. The chapter also highlights the importance of micro electro-mechanical systems (MEMS) in detecting and measuring physical parameters, contributing to the functionality of drones and aircraft.

1.3.1. Internet of Things

Generally speaking, IoT refers to the networked interconnection of everyday objects, which are often equipped with ubiquitous intelligence. IoT will increase the ubiquity of the Internet by integrating every object for interaction via embedded systems, which leads to a highly distributed network of devices communicating with human beings as well as other devices.

The fundamental concept of the proposed framework to protect drones lies in the fact that mobile semiautonomous devices are expected to enter the IoT architecture as another type of smart devices and, due to their significant impact on several everyday activities (sensitive/critical or not), they require well-established and high-quality security support. On this ground, the proposed framework envisions to provide the necessary security components that would facilitate the process of interconnecting drones and UAVs under the umbrella of the IoT, while exhibiting advanced intelligence and self-management characteristics(Lagkas et al., 2018).

5G and IoT Sensor Technologies for UAVs The 5G technology is expected to enhance mobile broadband, enable applications that require ultrareliable very low latency and very high availability networks, improve traffic safety and control, support industrial applications, remote manufacturing, training, surgery, logistics, tracking, and fleet management. It will be utilized for smart agriculture, precision farming, smart buildings, smart meters, support of 4K/8K UHD broadcasting, virtual and augmented reality without range limitations, including homes, enterprises, and large venues offering massive and critical Machine-To-Machine-Type Communications (MTMC) (Wang et al., 2012). This type of device communications can be integrated with typical Human-Type Communications (HTC) through suitable gateways in the context of a 5G architecture, as presented in Reference(Sarigiannidis et al., 2017) and illustrated in Fig.3.

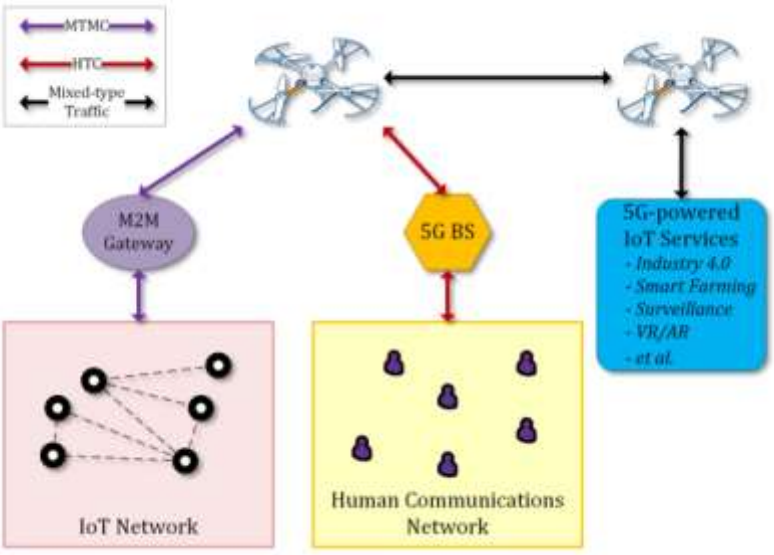

Fig.3. Unmanned aerial vehicle (UAV)-enhanced 5G-enabled Internet of Things (IoT) services (Lagkas et al., 2018).

1.3.2 Wireless Integrated Networked Sensors

In traditional airplane monitoring system (AMS), data sensed from strain, vibration, ultrasound of structures or temperature, and humidity in cabin environment are transmitted to central data repository via wires. However, drawbacks still exist in wired AMS such as expensive installation and maintenance, and complicated wired connections. In recent years, accumulating interest has been drawn to performing AMS via airborne wireless sensor network (AWSN) system with the advantages of flexibility, low cost, and easy deployment(Gao et al., 2018).

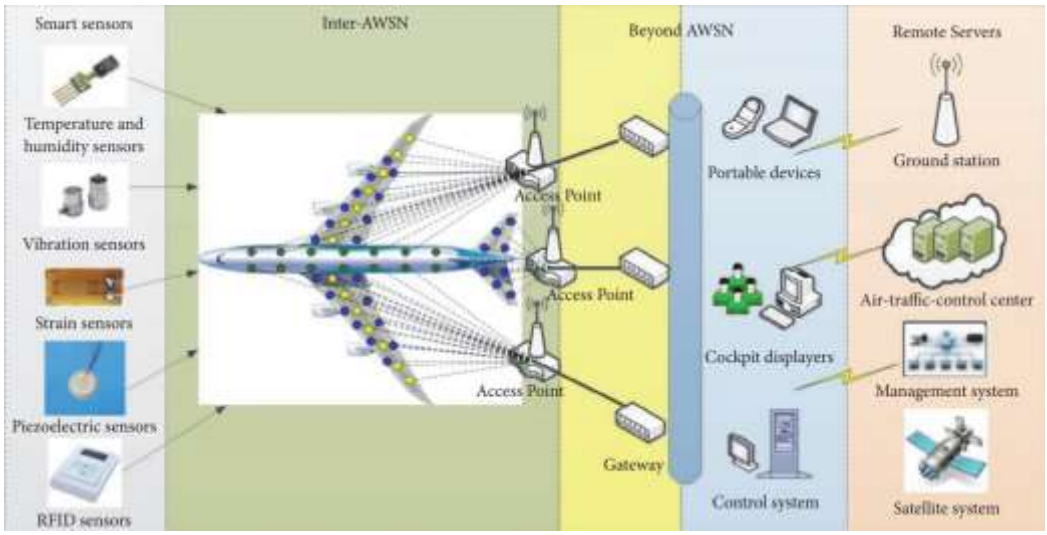

Fig. 4: The airborne wireless network schematic diagram(Gao et al., 2018).

As shown in Fig 4, The AWSN communication system includes four components: smart sensors, inter-AWSN, beyond AWSN, and remote servers. Within AWSN, various smart sensors deployed on airplane connect to airborne wireless sensor nodes. It is clear that the AWSN is formed among all sensor nodes depending on wireless transceivers.

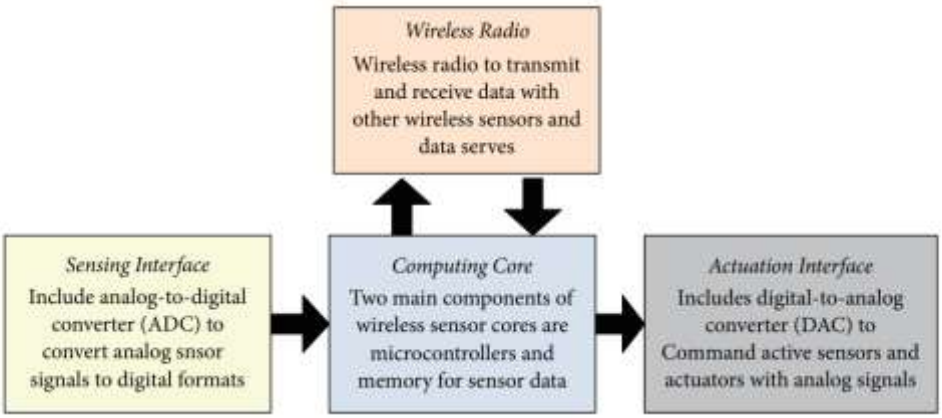

Fig. 5 The schematic diagram of airborne wireless sensor board (Gao et al., 2018)

The WINS network must interact with the external world. Fig. 6 shows a notional WINS system architecture wherein WINS nodes communicate with the external world via an enterprise level network, such as a factory control network and/or the internet. Two-way communication is provided throughout the system as an essential attribute (Zhu et al., 2020).

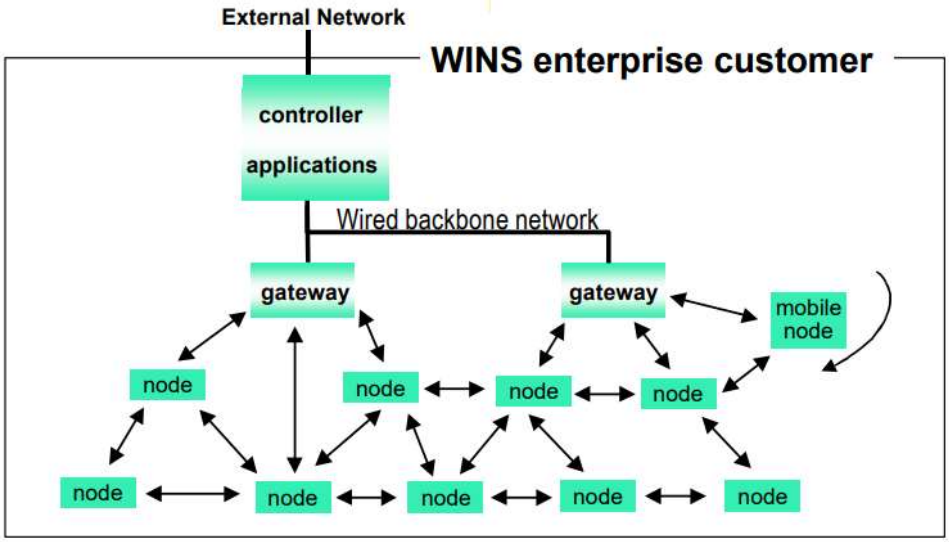

Fig. 6. A schematic description of a WINS system architecture(Marcy et al., 1999).

The Deployment of AWSN in AMS. General aircraft body is consisted of left and right wing, cockpit or cabin, engine, vertical tail, left and right horizontal stabilizer, landing gear, front, middle, and rear sections which are installed in subsystems of aircraft. Due to the dispersing deployment characteristic of the subsystems, cluster-star network topology is more suitable for AWSN in AMS (Sanjiv Rao & Vallikumari, 2012). Fig. 6 illustrates how the WSN is deployed inside cabin, fuel tank, on the wings and other sections of the airplane with clusterstar topology. To meet the requirements of AMS, one or more clusters are constructed in each subsystem or respective region of aircraft body, and cluster head and sensor nodes in each cluster formed cluster topology. The deployment of sensor nodes at certain optimum locations inside airplane enumerates as follows:

(1) *Fuel Tank.* The sensor nodes are deployed inside fuel tanks which are located in the wings and tail of the airplane to measure the level of fuel.

(2) *Exhaust*. Sensors placed inside the exhaust would monitor whether any obstructions exist in it.

(3) *Wheels.* The routine examination for health and condition of the wheels should be implemented before takeoff and after landing of aircraft. Moreover, the wheels might be also damaged while the aircraft is on the runway or in the air.

(4) *Engine*. The engine is the “heart” of an airplane, which should be monitored in real-time. Overheating or physical damage of the engine is harmful for airplanes. Most severe catastrophic

failures even airplane crashes are associated with the safety of engine. Tus, sensor nodes installed in and around the engine would monitor temperature and state of the engine surrounds and all components.

(5) *Wings*. Wings in the aircraft are always exposed to corrosion, impact, and crack damage due to external various complicated climatic environments. Sensor nodes installed in the wings would monitor vibration or strain arising from them to diagnose or forecast the localization, severity of them.

(6) *Fire and Safety*. Certain areas inside the airplane such as the aircraft cabin and the passenger area carry items like luggage, cockpit, the kitchen, passenger section, and the cargo, where smoke sensor nodes might detect free indication and send alerts through the AMS.(Gao et al., 2018)

The wireless airborne devices inevitably face interference due to elements of the harsh environment such as heavy dust, vibration, heat, freeze, uncertain temperature and humidity, bad weather in upper air, and other RF signals (Turkrnani & de Toledo, 1993), which contravene wireless communication principles.(Gao et al., 2018)

Use Cases for Wireless Networking with UAVs The use of UAVs as key entities of next-generation wireless networks constitutes one of the most promising applications of the corresponding technologies. A number of promising use cases are thoroughly detailed in Reference (Mozaffari et al., 2019) and presented below.

• UAV-carried flying base stations that complete heterogeneous 5G systems to enhance the coverage and capacity of existing wireless access technologies.

• UAV-based aerial networks that allow reliable, flexible, and fast wireless connections in public-safety scenarios.

• UAVs that support terrestrial networks for disseminating information and enhancing connectivity.

• UAVs as flying antennas that can be deployed on demand to enable mmWave communications, massive MIMO, and 3D network MIMO.

• UAVs that are used to provide energy-efficient and reliable IoT uplink connections.

• UAVs that form the backhaul of terrestrial networks to allow agile, reliable, cost-effective, and high-speed connectivity.

• UAVs able to cache popular content and efficiently serve mobile users by following their mobility patterns.

• UAVs that act as users of the wireless infrastructure for surveillance, remote-sensing, and virtual-reality cases, and package-delivery applications.

• UAVs that collect vast amounts of city data and/or enhance cellular network coverage in a smart-city scenario(Lagkas et al., 2018)

1.3.3 Magnetoresistive Sensors

Lord Kelvin discovered magnetoresistance in 1857 when he noticed the slight change in the electrical resistance of a piece of iron when he placed it in a magnetic field. But it took more than 100 years before a first magnetoresistive (MR) sensor concept was reported by Hunt in 1971. And it lasted additional 20 years for IBM to introduce the first MR head, which used a strip of magnetoresistive material to detect bits, into a hard disk drive in 1991. Earlier, MR sensors were used in less demanding applications of price tag and badge readers (read-only) and magnetic tape (1985) (TE Connectivity, n.d). MR sensors tend to consume less power, and they are smaller in size than the Hall-effect sensors(Zhu et al., 2020).

1.3.4 Micro Electro-Mechanical Systems

MEMS, or microelectromechanical systems, are commonly characterized as minuscule devices that are deliberately designed, manufactured, and employed to engage with and effect modifications within a specific vicinity (Walraven, J., 2003). These devices have the capacity to respond mechanically, electrically, or chemically to external stimuli, thereby generating a corresponding mechanical, electrical, or chemical reaction within their immediate surroundings (Mishra et al., 2016). These compact and highly advanced devices possess enhanced cognitive, operational, sensory, and communicative capabilities, rendering them increasingly prevalent in a wide array of traditional applications, where they are gradually supplanting their larger-scale counterparts (Walraven, J., 2003).

MEMS components are classified into six distinct applications, encompassing the following categories:

- Sensors
- Actuators
- RF MEMS

- Optical MEMS
- Microfluidic MEMS
- Bio MEMS

MEMS, in the context of Integrated Vehicle Health Management, play a pivotal role in the functioning of accelerometer and gyroscope sensors. These sensors are key components of MEMS, which are designed to detect and interact with their surrounding environments.

Accelerometer

For a comprehensive understanding of integrated vehicle health management systems concerning UAVs and autonomous aircraft models considerations must be given to analyzing accelerometers' measurements carefully. The reason being that such an evaluation provides us with valuable insights into their reliability quotient as well as any potential maintenance requirements they may need over time.The outcome supports formulating more robust vehicle health monitoring strategies intended at promoting efficient functioning throughout operations.In this particular segment of our study report,the outcomes from comparing & discussing spectrograms obtained from raw and processed data, are presented.

The accelerometer serves as an automated instrument utilized for quantifying acceleration, detecting and measuring vibrations, and gauging the acceleration induced by physical movements or inclinations of an object. The utilization of accelerometers extends to the measurement of vibrations in diverse contexts such as automobiles, engines, buildings, and security installations (Faisal et. al. 2019). Accelerometers have diverse applications beyond their traditional use in measuring physical motion. In more advanced applications, a wide range of sensors is available for navigation purposes. One such sensor is the accelerometer, which is capable of measuring acceleration, a fundamental parameter in motion analysis. Accelerometers have gained substantial usage in contemporary automotive systems, serving diverse functionalities such as enabling airbag deployment during collisions. Additionally, these sensors find application in various consumer electronic devices like game controllers, personal media players, cell phones, and digital cameras (Mishra et al., 2016). Acceleration refers to the rate of change of velocity over time and can be positive (resulting in increased speed) or negative (resulting in decreased speed, known as deceleration). The direction or orientation of the acceleration is also significant as it represents a change in the vector quantity of velocity. Acceleration can be influenced by changes in the direction of movement, adding to the complexity of the analysis (Faisal et. al., 2019).

To obtain distance data from an accelerometer sensor, a dual integral process is required to integrate the output of the sensor. Researchers and developers are currently exploring various applications of accelerometer sensors, such as detecting foot movements for navigation purposes and utilizing motion for console gaming or other control functions. These advancements in accelerometer sensor technology open up possibilities for enhanced navigation systems and interactive user experiences in various domains(Faisal et. al., 2019).

Fig. 7 . Accelerometer (PNGWing, n.d.)

Principle of Accelerometer

In a simplified manner, the MEMS accelerometer can be conceptualized as a system governed by Newton's second law, where a mass is affixed to a spring within a defined reference frame (Fig. 8).

This basic configuration encompasses two primary principles of MEMS accelerometers: one involves the measurement of mass displacement, while the other entails monitoring the frequency variations of a vibrating element caused by tension alterations. The accelerometer is capable of quantifying linear acceleration, and by performing double integration of the acquired signal, positional information can be obtained (Grahn, 2017).

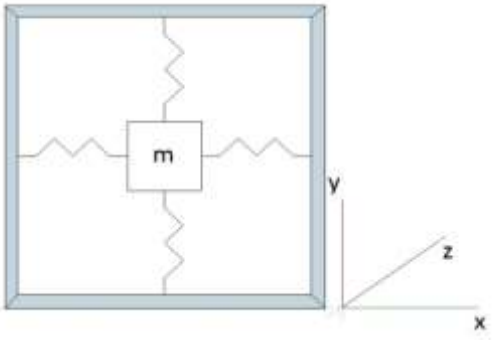

Fig. 8. Illustration of the basic principle of Newton's second law in two dimensions where a mass m is attached to springs within a reference frame (Grahn, 2017)

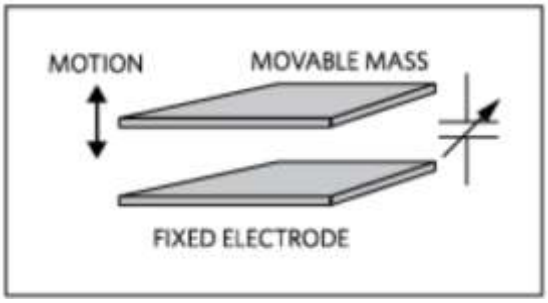

Fig. 9 . Moving mass and capacitance(Dadafshar, 2014)

Capacitance sensing is a widely adopted methodology for accelerometer sensing, wherein the measurement of acceleration is closely associated with the alteration in capacitance of a movable mass (Fig. 9). This sensing technique is renowned for its remarkable precision, stability, minimal power dissipation, and straightforward construction. Additionally, it exhibits resistance to noise and temperature-induced fluctuations. The bandwidth of a capacitive accelerometer is typically limited to a few hundred Hertz due to the inherent physical characteristics of its geometry, particularly the spring structure, and the presence of enclosed air within the integrated circuit, which functions as a dampening agent (Dadafshar, 2014).

$$C = \frac{\varepsilon_r \times \varepsilon_0 \times A}{D} (\text{Farad})$$

ε_0 = Permitted free space

A = Area of overlap between electrodes

D = Separation between the electrodes

ε_r = Relative material permitted between plates

Gyroscope

A gyroscope is a device mounted on a frame that can sense the angular velocity of the frame when it rotates (Faisal, et.al., 2019). Gyroscopes(Figure 9) can be classified into various categories based on their operational principles and technological applications. They can serve as standalone devices or be integrated into complex systems such as Inertial Measurement Units (IMUs), gyrocompasses, attitude heading reference systems, and navigation systems (Passaro et al., 2017).

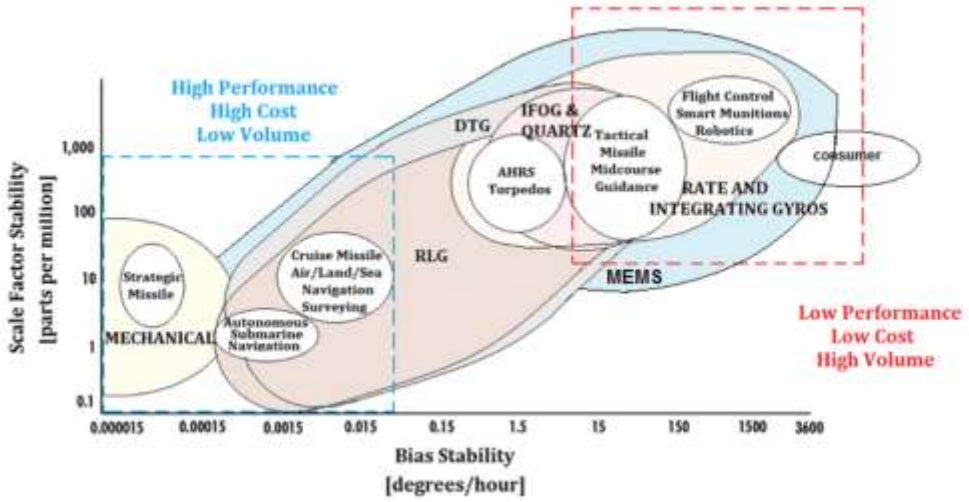

Fig. 10 Scale factor stability (i.e., the accuracy of the gyroscope in monitoring the sensed angular velocity), expressed in parts per million (ppm), as a function of the bias stability (intrinsically dependent on the gyroscope technology) for Mechanical Gyroscopes, Ring Laser Gyroscopes (RLG), Interferometric Fiber-Optic gyroscopes (IFOG), Quartz, Dynamically Tuned Gyroscopes (DTG), Rate and Integrating Gyroscopes and MEMS (Passaro, V., 2017).

Historically, mechanical gyroscopes have been in use since the 19th century. They can be classified into displacement gyroscopes and rate gyroscopes. These gyroscopes consist of a rotor in the shape of a toroid that rotates around its axis. On the other hand, optical gyroscopes, which have been in use since the 20th century, operate by detecting the difference in the time it takes for counter-propagating laser beams to travel in opposite directions along a closed or open optical path. In Fig. 10, the left-bottom spectrum represents mechanical gyroscopes, while the middle spectrum represents optical gyroscopes. The most commonly used types of optical gyroscopes are IFOG (Interferometric Fiber Optic Gyroscope) and RLG (Ring Laser Gyroscope), both of which utilize the principles of the Sagnac effect. Among these gyroscopes,

the ring laser gyroscope is currently more prevalent and holds a larger market share, particularly for applications that require very high performance (Passaro, V., 2017).

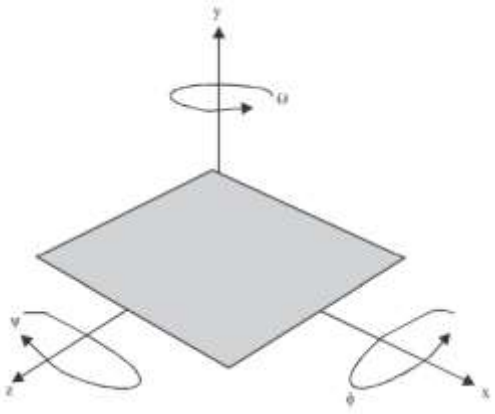

Fig. 11. Illustration of the basic principle of a gyroscope and how the rotations (ψ,θ,ϕ) occur around respective axes (Passaro et al., 2017).

1.4. Applications

The applications of unmanned aerial vehicles are diverse, including areas related to civilian, military, commercial, and governmental sectors (Merwaday & Guvenc, 2015; Motlagh et al., 2017). Examples include environmental monitoring (e.g., pollution, health of plants, and industrial accidents) in the civilian sector. In military and governmental areas, we mainly have surveillance and delivery applications aiming to acquire or provide information at locations after a disaster or attack, and to distribute medicine or other essential items. Commercial applications are focused on delivering products and goods both in urban and rural areas. UAVs, since they are dependent on sensors, antennas, and embedded software, are considered as part of the Internet of Things, providing a two-way communication for applications related to remote control and monitoring (Luo et al., 2015).

The Internet of Things (IoT) constitutes a rapidly emerging cutting-edge environment in which the focal concept lies in the orchestration of a large variety of smart objects in such a way that they can be utilized and operated globally, either directly by users or by special software that captures their behavior and objectives. IoT enables objects to become active participants of everyday activities, with numerous promising applications through various communication technologies in the context of the “smart-city” vision (Zanella et al., 2014).

The wireless airborne devices employed inside airplane forward structural or environmental data to data aggregation center. Unfortunately, the electromagnetic waves from devices inside internal airplane should penetrate complex metallic and composite spaces. For instance, wireless propagation in airplane wing suffers from high attenuation as it goes through wing relief holes and spaces between wing structures including skin, spar, stringers, and ribs. However, path loss models for airplane wing environment link have been seldom investigated. It is challenging to get complete wireless link budget due to the high metallic feature of airplane wing. Due to the particularity of airplane wing environment, traditional path loss models for building or outdoor environments (e.g., alfsh-Ikegami (Ruff et al., 2004), Keenan-Motley (Cummings et al., 2007), and Turkmani (Arslan, 2009)) are unsuitable for empirical path loss of airplane wing(Gao et al., 2018).

Utilizing an IVHM system proves to be a commendable strategy when it comes to the management and production of vehicle platforms and to ensure cost-effective field operations throughout the life cycles of advanced spacecraft, significant modifications are implemented. Intelligent technology, employed by an IVHM system, is utilized in both existing and new vehicles to facilitate cost-effective decision-making regarding usage, support, and design. This serves as the current rationale supporting the adoption of IVHM.

Conclusion of Literature Review

In conclusion, the literature review highlights the diverse applications and characteristics of UAVs and IVHM systems in the aerospace. Sensor technologies play a crucial role in UAVs, enabling functions such as condition monitoring, geographical mapping, and dangerous task execution. Various sensors, including accelerometers, tilt sensors, engine intake flow sensors, magnetic sensors, and current sensors, contribute to the overall health and safety of UAV operations. Current sensors, in particular, are essential for preventing overcharging, monitoring battery energy consumption, and providing real-time measurements for system fault detection and protection.

Integrated System Health Management (ISHM) systems, encompassing diagnostic and prognostic functions, are essential in aerospace, defense, and transport systems. IVHM aims to enhance decision-making, improve maintenance programs, reduce costs, and enhance the availability of aircraft. Over the years, IVHM has evolved with advancements in digital systems, built-in test circuits, and data-driven approaches. The current decade witnesses the integration of big data analysis, cloud-based computing, and robotics to improve real-time health monitoring and maintenance.

Overall, the reviewed literature emphasizes the importance of sensor technologies, and IVHM systems in ensuring the efficient operation, safety, and maintenance of aerospace systems.

2. Methodology

This section presents the methodology employed to analyze the flight logs of the unmanned aerial vehicle (UAV) in the context of this research. The flight logs, obtained from the university and recorded during a specific flight, serve as the primary data source for this analysis. The methodology comprises the following steps: data conversion, data examination, and graphical analysis. The methodology employed in this research is based on data-driven reasoning techniques, which involve assigning mathematical models and weight parameters to the observed variables of the system.

2.1 Data Conversion

The flight logs, initially provided in a proprietary format, are converted into MATLAB files using Mission Planner. Mission Planner is a widely used software tool specifically designed for UAV mission planning and analysis. By converting the logs into MATLAB files, the data becomes readily accessible for further analysis and processing.

2.2 Data Examination

Instead of using a physical model as in the case of model-based reasoning, data-driven reasoning techniques calculate and assign mathematical models and weight parameters to the observed variables of the system using a training dataset previously gathered from the system (Ranasinghe et al., 2022).

This approach is powerful in predicting near-future behaviours because it focusses on identifying trends in the data. This is particularly useful near the end of life of a component, as the trends show distinct characteristics at this stage (An et al., 2015).

Once the flight logs are converted into MATLAB files, the focus shifts to examining the data contained within. Specifically, this analysis focuses on the accelerometer and gyroscope data. Each of these sensor types consists of three channels, resulting in a total of six data streams for analysis. The MATLAB files contain 133,961 data points, capturing a comprehensive dataset for investigation.

During the data examination phase, the recorded data is processed using MATLAB's built-in functions and custom scripts. Statistical analysis techniques, signal processing algorithms, and data visualization methods are applied to explore the characteristics and patterns within the recorded sensor data.

2.3 Graphical Analysis

As an integral part of the analysis process, graphical analysis plays a crucial role in presenting and interpreting the results. MATLAB's extensive range of graphical capabilities and add-ons are utilized to create visual representations of the analyzed data. By employing appropriate visualization techniques, such as line plots, scatter plots, histograms, and spectrograms, the findings are visually represented and effectively communicated.

The graphical analysis is instrumental in identifying trends, anomalies, correlations, and other relevant insights within the accelerometer and gyroscope data. These visual representations serve as a basis for further interpretation and formulating conclusions based on the analysis outcomes.

2.4 Functions and Formulas

In this section, the functions and formulas utilized in the processing and analysis of the data obtained from the UAV's accelerometer and gyroscope are presented. A crucial role is played by these functions and formulas in preprocessing the data, applying mathematical operations, filtering, normalizing, and extracting useful information from the raw sensor readings. Additionally, the specific functions and their purposes are described, as well as the notation and terminology used in this thesis. These tools enable insights to be gained into the characteristics of the sensor data and facilitate subsequent analysis and interpretation. Through the application of these functions and formulas, the raw data can be transformed into meaningful representations, paving the way for further investigation and exploration.

Data = The combined readings from the accelerometer and gyroscope sensors on the UAV are collectively referred to as the "UAV sensor data." It includes three sets of measurements: AccX, AccY, and AccZ for the accelerometer, and GyrX, GyrY, and GyrZ for the gyroscope.

$\mathrm{Norm}_{\mathrm{Data}}$ = Normalized data

$\mathrm{Mean}_{\mathrm{Data}}$ = *Mean of normalized data*

$\mathrm{Std}_{\mathrm{Data}}$ = Standard deviation of the normalized data

$\mathrm{Data}[R \notin I]$ = Denotes the submatrix of Data containing only the rows whose indices are not in the set I.

R = Collection of all the possible indices that can be used to access the rows of Data.
N = Number of normalized data set

f = Frequency vector (Hz)

fc = Cutoff frequency

fs = Sampling frequency

fft = Fast Fourier Transform

$\text{Data}_{\text{fft}} =$ FFT of the data

$\text{Data}_{\text{fft}_{\text{mag}}} =$ Magnitude of the FFT

unique = Removing duplicate rows while preserving the order.

fillmissing('linear') = Filling missing values in Data using linear interpolation

fillmissing('spline') = Filling missing values in Data using spline interpolation

$$\text{Data} = \text{unique}(\text{Data}, 'rows', 'stable')$$

$$\text{Data} = \text{Data}[\text{R} \notin \text{I}]$$

$$\text{Data} = \text{fillmissing}(\text{Data}, 'linear')$$

$$\text{Data} = \text{fillmissing}(\text{Data}, 'spline')$$

$$[b, a] = butter\left(2, \frac{f_c}{\left(\frac{f_s}{2}\right)}\right)$$

$$Data = filtfilt(b, a, Data)$$

$$Norm_{data} = \frac{Data}{\sqrt{\sum(Data^2, 2)}}$$

$$Mean_{Data} = \frac{1}{N}\sum_{i=1}^{N} Norm_{Data}$$

$$Std_{Data} = \sqrt{\frac{1}{N}\sum_{i=1}^{N}(Norm_{Data_i} - Mean_{data})^2}$$

$$N = \text{size}(\text{GyrData}_{\text{norm}}, 1)$$

$$f = \left(0{:}\frac{N}{2}\right)\left(\frac{\text{fs}}{\text{N}}\right)$$

$$\text{Data}_{\text{fft}} = \text{fft}(\text{Data}_{\text{norm}})$$

$$Data_{fft_{mag}} = \frac{\left|Data_{fft}\right|}{N}$$

$$Data_{fft_{mag}} = Data_{fft_{mag}}(1 : floor(N/2) + 1, :)$$

The following functions were used in the processing and analysis of the data in this study:

- 'unique': This function was utilized to remove duplicate rows from the dataset. The 'rows' and 'stable' options were specified to ensure that the rows were removed in the same order as they appeared in the original data.
- 'isnan': This function was used to check if any element in the matrix was NaN (Not-a-Number) and returned a logical array of the same size.
- 'any': The 'any' function was utilized to determine if any element of the matrix was nonzero, returning a logical value.
- 'fillmissing': This function was used to replace NaN values in the matrix with interpolated values based on the specified method, either 'linear' or 'spline'.
- 'butter': The 'butter' function was used to design a Butterworth filter with the specified cutoff frequency (fc) and order (2 in this case).
- 'filtfilt': This function was used to apply the designed Butterworth filter to the data using zero-phase filtering. The filter coefficients and the data were provided as input.
- 'sqrt': This function was used to compute the square root of each element in the matrix.
- 'sum': The 'sum' function was utilized to compute the sum of each row in the matrix.
- 'corrcoef': This function was used to compute the correlation matrix for the accelerometer and gyroscope data.
- 'kmeans': The 'kmeans' function was used to perform k-means clustering on the gyroscope data.
- 'silhouette': This function was utilized to compute the silhouette scores for each data point in the gyroscope data.
- 'scatter3': This function was used to create a 3D scatter plot of the gyroscope data.
- 'max': The 'max' function was utilized to return the maximum element in the array.
- 'fprintf': This function was used to print a formatted message to the console.
- 'fft': The 'fft' function was utilized to compute the discrete Fourier transform (DFT) of the data.
- 'abs': This function was used to compute the absolute value of each element in the matrix.

- 'spectrogram': Finally, the 'spectrogram' function was used to compute the spectrogram of the data using a sliding window and overlapping segments. This function takes in the data, window size, overlap, and sampling frequency (fs) as input.

These functions were instrumental in processing and analyzing the data for this study, enabling various data manipulation, filtering, statistical analysis, clustering, and visualization tasks.

3. Results

This section presents the results of analyzing accelerometer and gyroscope data from the university's UAV. The analysis includes spectrogram analysis, determination of the optimal k value, and clustering results.

3.1 Accelerometers and Gyroscope sensors analysis

This analysis aims at understanding how accelerometer and gyroscope readings lend themselves towards integrated vehicle health management systems designed for use in autonomous aircrafts or unmanned aerial vehicles. It does so by analyzing different aspects related to their performance such as behavior which plays an essential role in effective vehicle monitoring/maintenance practices.

We deployed a spectrogram technique designed for examining time-frequency characteristics of signals from both raw sensor output as well pre-processed readings given that interpreting raw data can be challenging leading often times into errors associated with false assumptions/misleading interpretations. By using processed data together with application of the spectrogram method allowed us clearly identify variations across different time intervals and frequency bands, hence providing a roadmap for comprehensive understanding of how the sensors perform under different operational scenarios.

The primary objective of this juxtaposition is to determine just how much effect processing techniques have on sensor data interpretation quality. Based on our evaluation of clarity and precision in the information extracted from signals courtesy of spectogram readings, we aim to establish the effectiveness level of these processing methods

Through the spectrogram analysis, we will investigate the time-frequency characteristics and patterns exhibited by the accelerometer and gyroscope data. This examination will enable us to gain insights into the dynamic behavior and performance of the unmanned aerial vehicles and autonomous aircraft under study.

By comparing the spectrograms of the raw and processed data, we will assess the extent to which data processing techniques contribute to the improvement of signal quality and the identification of relevant features. This analysis will help us determine whether the processed data provides a more reliable and meaningful representation of the underlying vehicle health status and performance.

The results of this comparative analysis will be presented in the form of graphical representations and accompanied by a detailed discussion of the observed differences and implications. We will highlight any significant findings or patterns that emerge from the comparison of spectrograms between the raw and processed data.

Through the analysis of these results, we contributed to the understanding of integrated vehicle health management systems in UAVs and autonomous aircraft, specifically focusing on the role of data processing in enhancing the analysis and interpretation of sensor data.

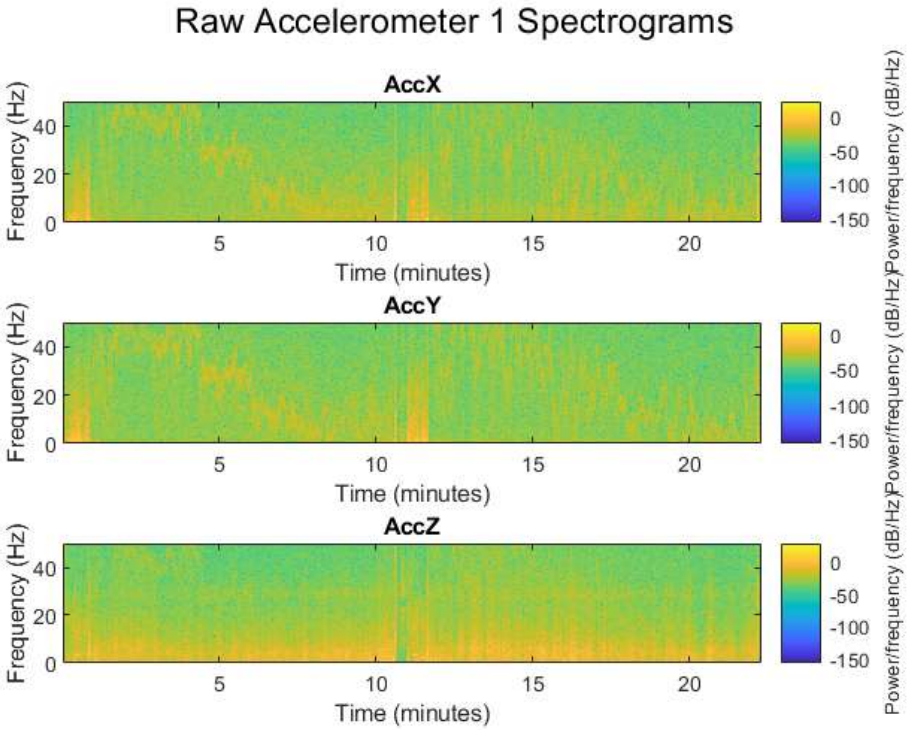

Fig. 12 Raw Accelerometer 1 Spectrogram

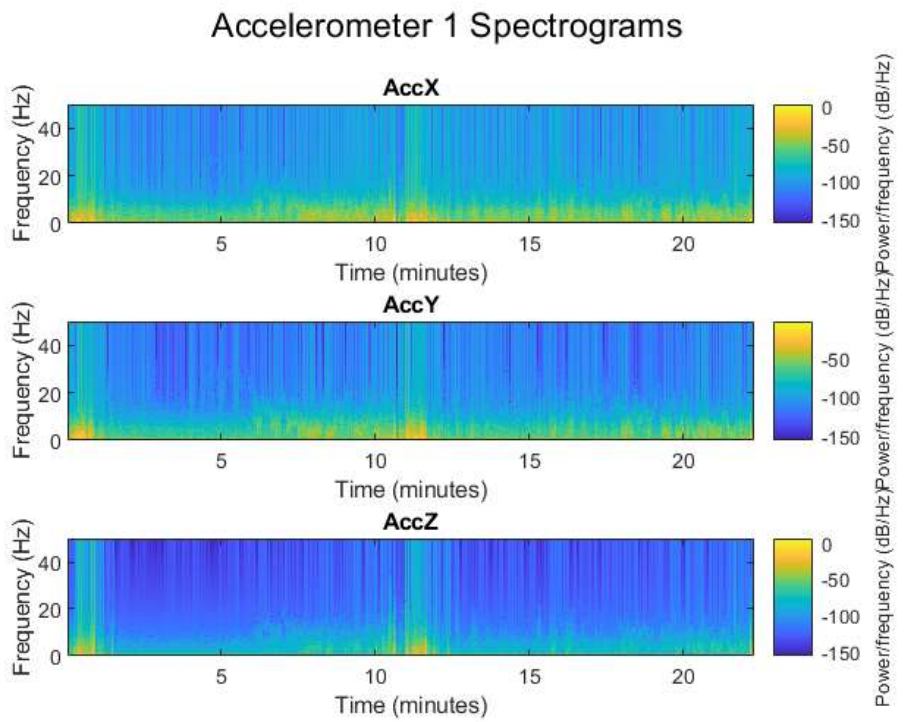

Fig. 13. Accelerometer 1 Spectrograms

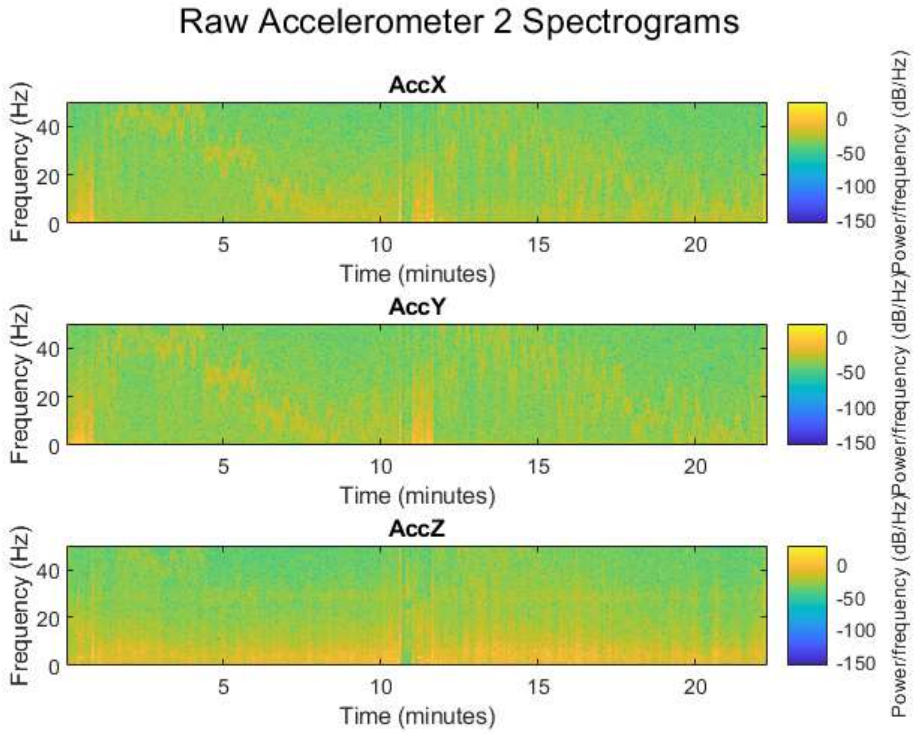

Fig. 14. Raw Accelerometer 2 Spectrograms

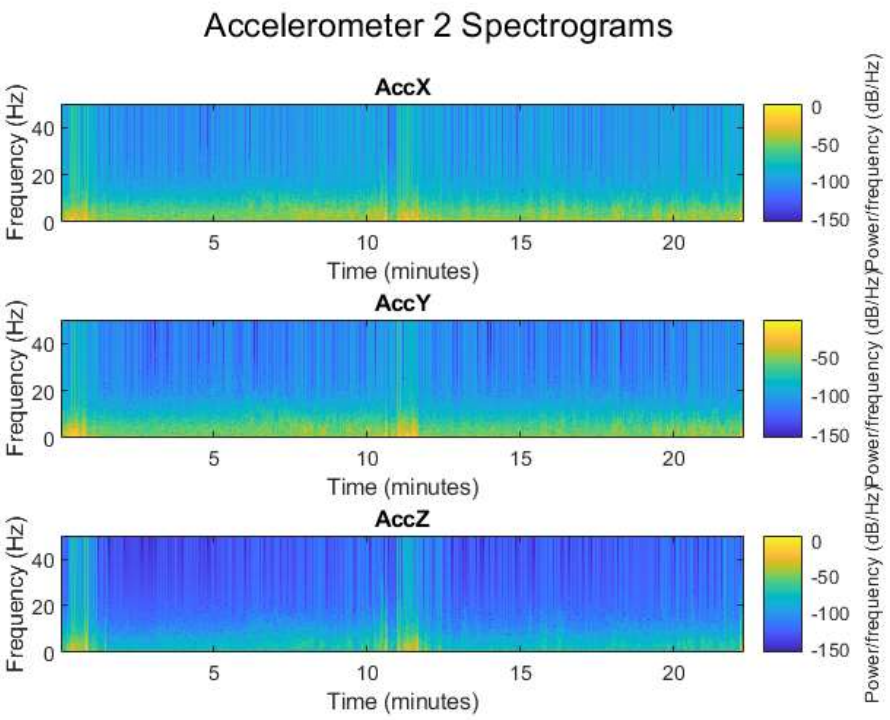

Fig. 15. Accelerometer 2 Spectrograms

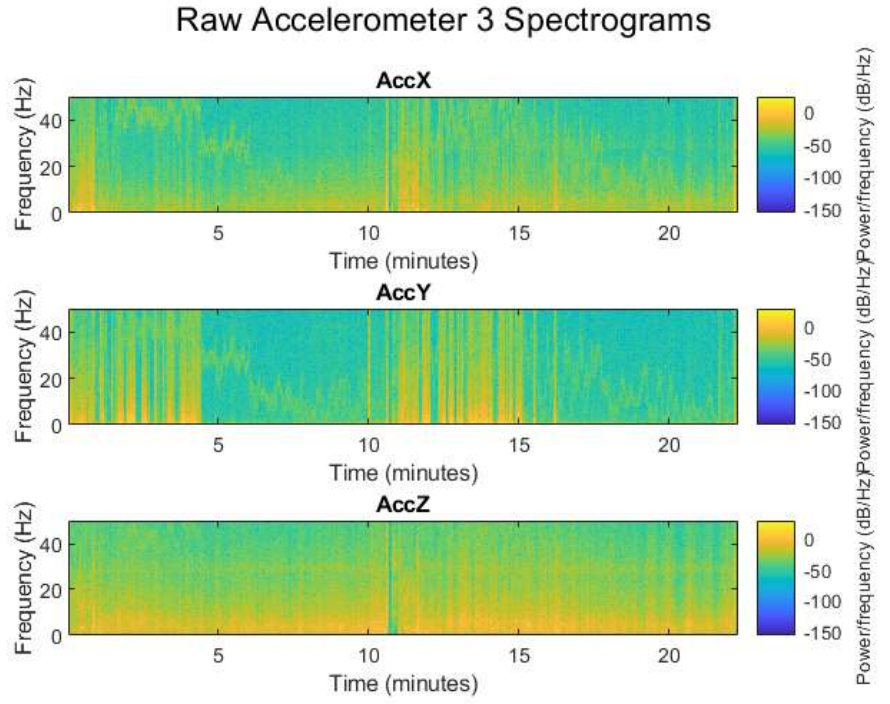

Fig. 16. Raw Accelerometer 3 Spectrograms

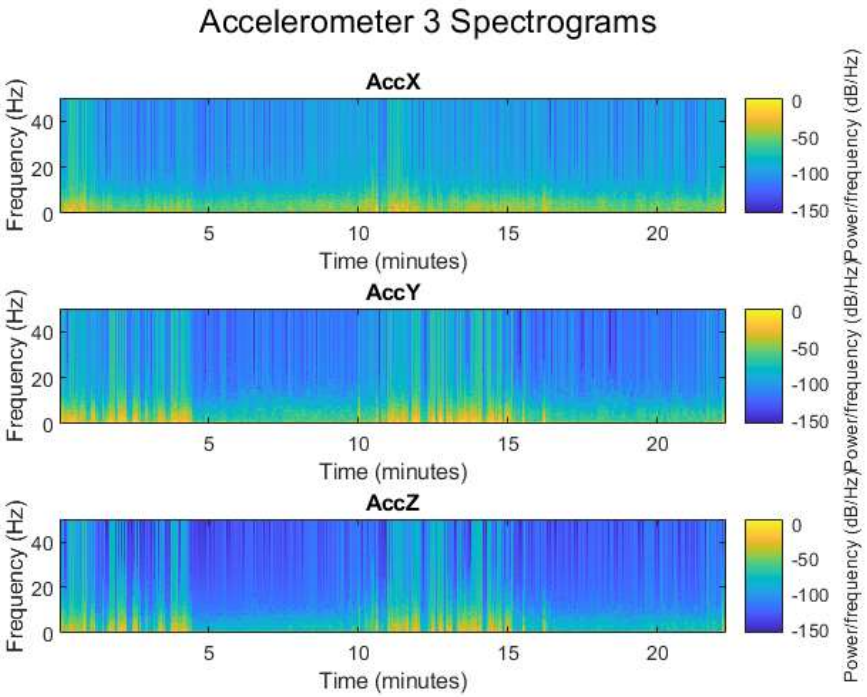

Fig. 17. Accelerometer 3 Spectrograms

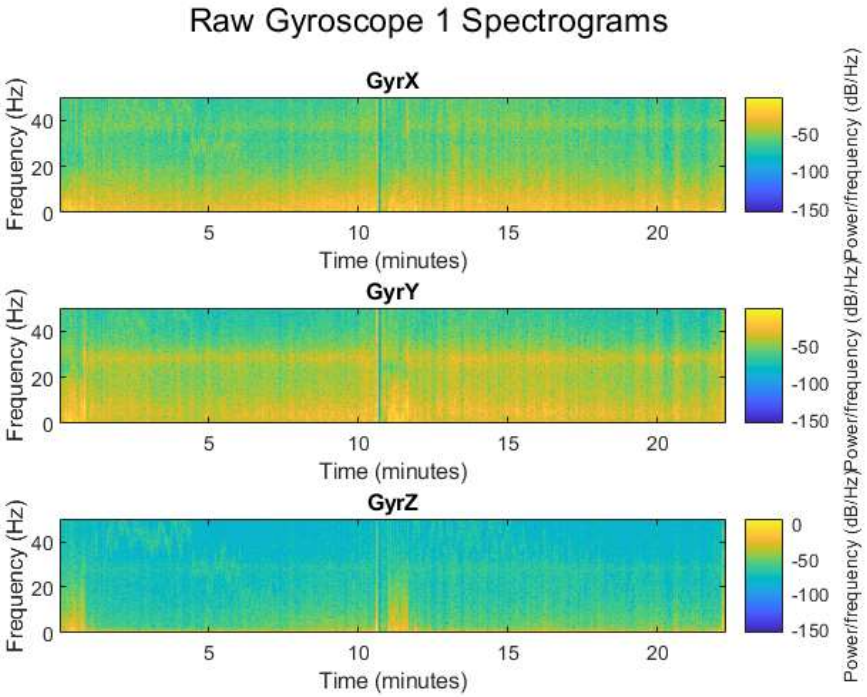

Fig. 18. Raw Gyroscope 1 Spectrograms

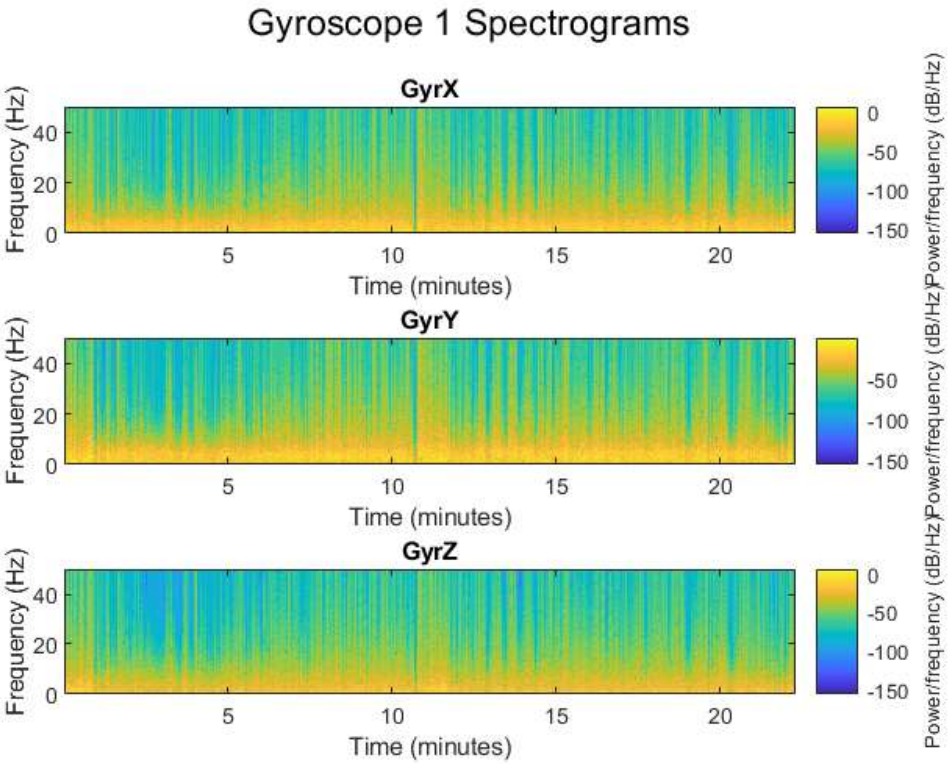

Fig. 19. Gyroscope 1 Spectrograms

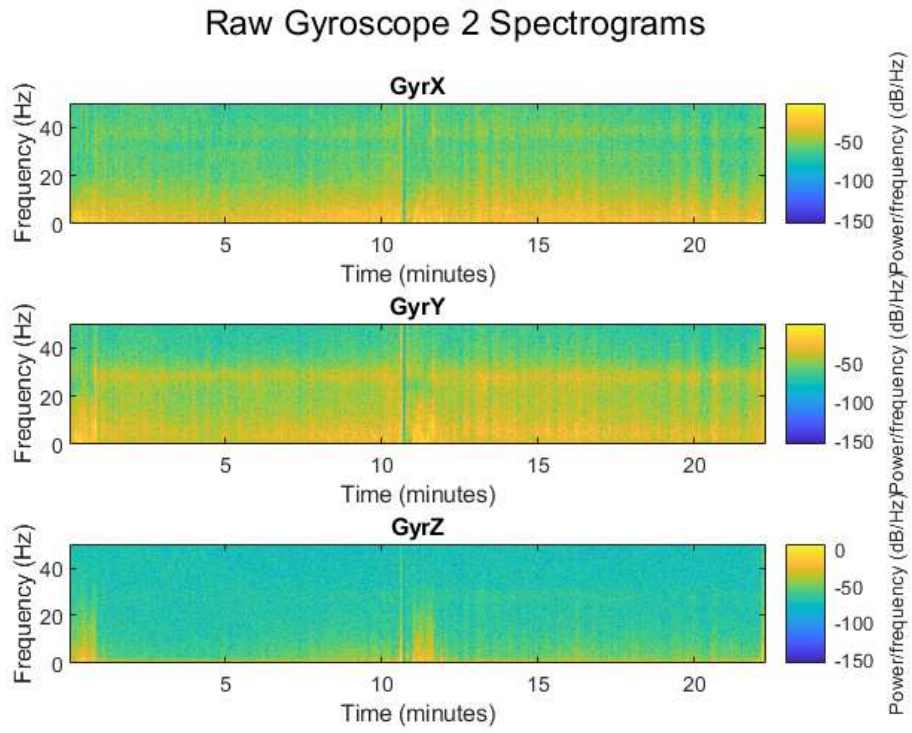

Fig. 20. Raw Gyroscope 2 Spectrograms

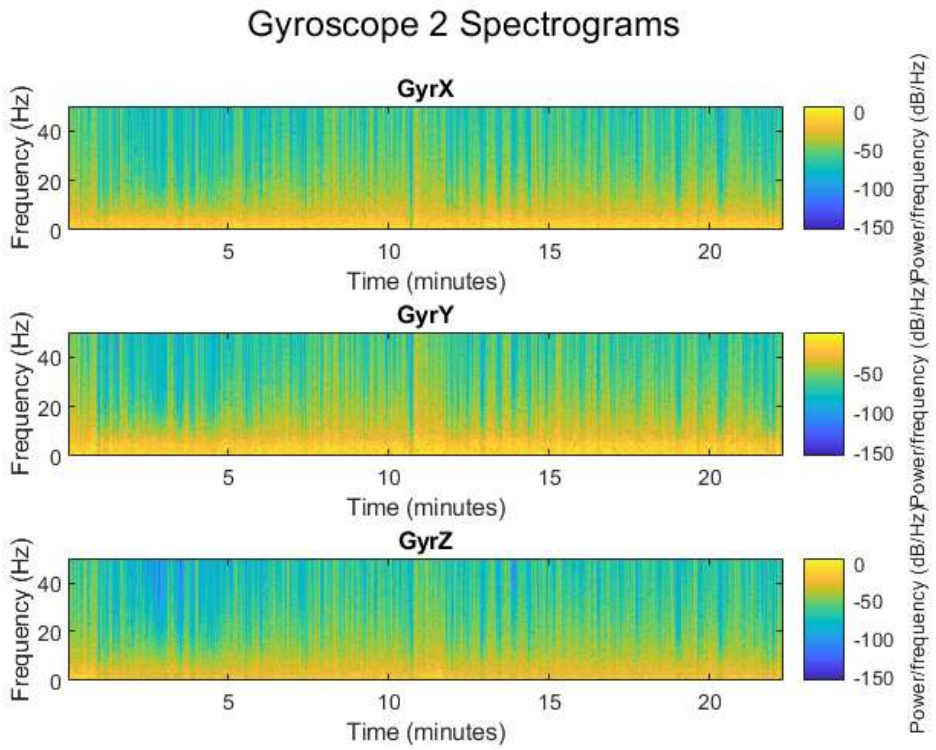

Fig. 21. Gyroscope 2 Spectrograms

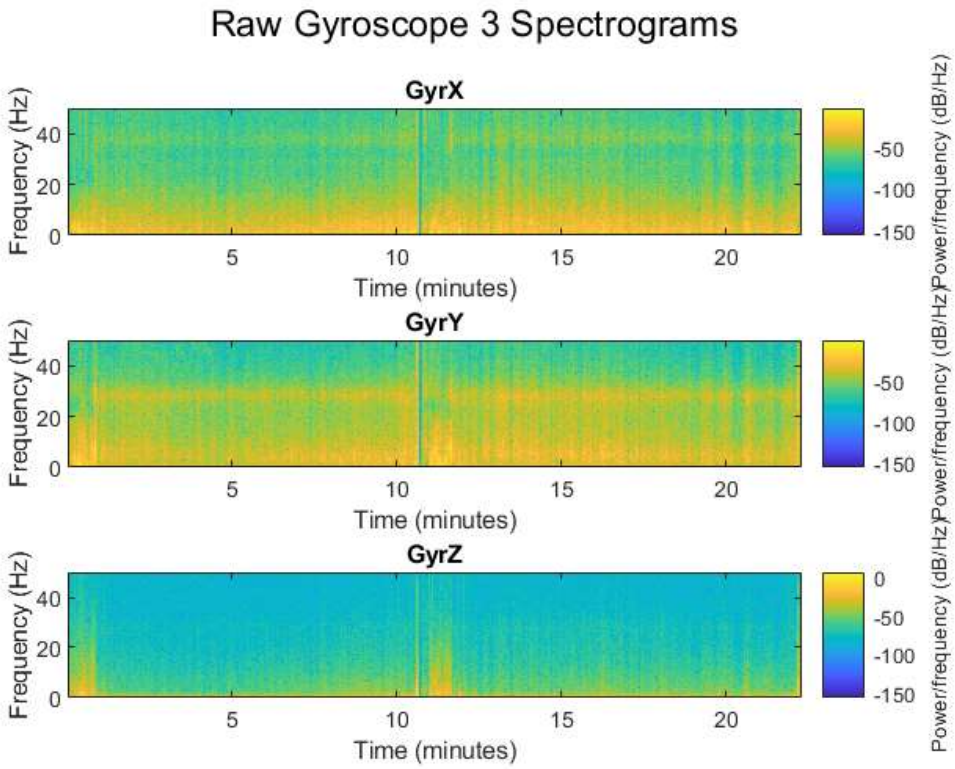

Fig. 22. Raw Gyroscope 3 Spectrograms

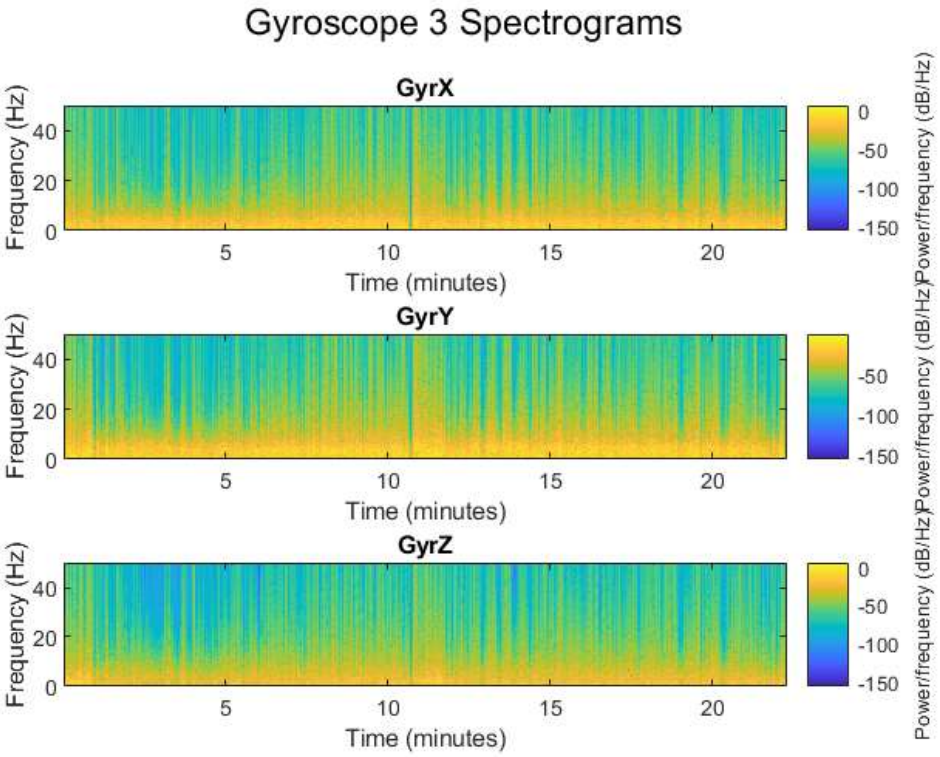

Fig. 23. Gyroscope 3 Spectrograms

When comparing the raw and processed data, a noticeable distinction arises. Upon observing the raw data (Fig. 12, 14, 16, 18, 20, 22), it becomes evident that the data itself is inherently noisy and lacks readability. Nevertheless, after undergoing processing, the spectrograms (Fig. 13, 15, 17, 19, 21, 23) exhibit discernible patterns and behaviors. Considering the fact that the observed data corresponds to a well-functioning flight, these measures can be employed as reference data for future investigations involving specific UAVs.

Upon careful examination of each processed spectrogram, notable occurrences of unusual movement can be observed at the initial and mid-flight stages. These instances can be attributed to specific factors: at the beginning, it signifies the commencement phase, while in the middle, it indicates a transition from autopilot to manual control. These insights provide valuable contextual understanding of the flight dynamics and aid in comprehending the behavior of the UAV during different operational phases. These states can also be observed through alternative platforms. Fig 24 depicts a graph obtained from plot.ardupilot.org, utilizing our flight log data. This additional representation corroborates the findings derived from the processed spectrograms, further validating the identified flight states and behaviors. The graph from plot.ardupilot.org serves as an external reference, reinforcing the consistency and reliability of our observations regarding the UAV's operational phases and transitions.

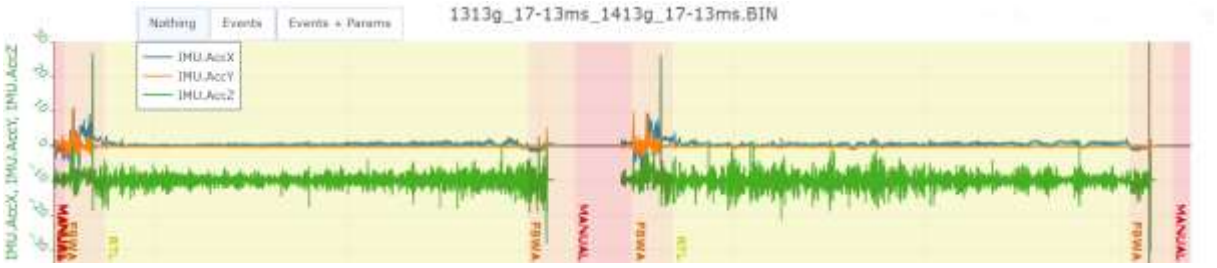

Fig. 24. Graph Accelerometer Graph from plot.ardupilot.org

3.2 Determining the Optimal Number of Clusters using Silhouette Score

To evaluate the appropriate number of clusters for the data analysis, the silhouette score method was employed. The resulting analysis revealed that the optimal number of clusters was determined to be 3, with an average silhouette score of 0.9553 (see Fig 25) . This high average silhouette score indicates the quality of the clustering results, suggesting well-defined clusters with relatively homogeneous data points within each cluster.

The silhouette score ranges from -1 to 1, where a score of 1 signifies that each data point is closely aligned with its own cluster and distantly related to neighboring clusters.

A score of 0 indicates that the data point lies on the boundary between clusters, while a negative score implies that the data point may be better suited to a different cluster.

Given the proximity of the average silhouette score to 1, it can be inferred that the clustering algorithm successfully grouped similar data points together, resulting in well-defined clusters. This finding highlights the effectiveness of the clustering technique in identifying and grouping data points with shared characteristics.

In the context of the thesis, it can be stated that the silhouette method was employed to determine the optimal number of clusters, and an average silhouette score of 0.9553 was obtained when utilizing 3 clusters. This score indicates favorable clustering results and the presence of relatively homogeneous data points within each cluster. These findings hold significant implications for the research, suggesting a successful analysis of the data and potentially paving the way for further investigations in the field.

Further discussions can focus on the implications of these findings for the integrated vehicle health management systems in unmanned aerial vehicles and autonomous aircraft, highlighting the potential applications and future directions for research in this area.

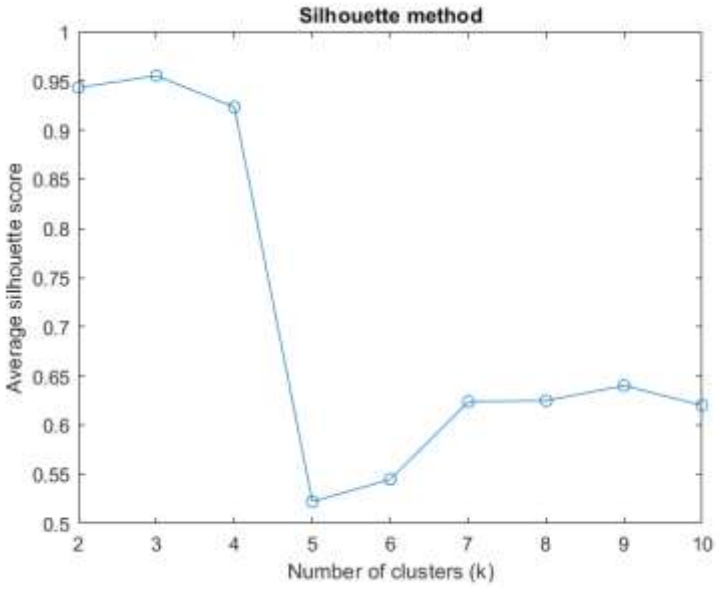

Fig. 25. Silhouette method graph for deciding **k** value

3.3 Clustering Results

The purpose of clustering analysis in this study was to identify meaningful patterns and groupings within the accelerometer and gyroscope sensor data obtained from flight logs of UAVs'. By employing clustering techniques, the data points were organized into clusters (Figure based on their similarity in order to gain insights into the behavior, performance, and health status of the vehicles.

In the context of this analysis, one of the key objectives was to detect anomalies within the sensor data. Anomalies can be characterized as data points that deviate significantly from the centroids of their assigned clusters or exhibit high variance compared to the other data points within their respective clusters. The identification of anomalies can be crucial for identifying unusual or potentially problematic behavior in the vehicles.

Upon conducting the clustering analysis, it was determined that there were no anomalies present within the accelerometer and gyroscope data. This suggests that the data points were well-aligned with their assigned clusters and exhibited consistent characteristics within each cluster. The absence of anomalies indicates that the sensor data was relatively consistent and did not display any unusual or abnormal patterns.

In the subsequent sections, graphical representations of the clustering results will be presented. These graphs provide visual insights into the distribution of the data points within their respective clusters and serve to illustrate the absence of anomalies. By examining these

graphs, it is possible to gain a better understanding of the clustering outcomes and verify the consistency and coherence of the sensor data within each cluster.

The graphical representations generated using MATLAB present a visual summary of the clustering analysis and provide valuable information regarding the grouping and organization of the accelerometer and gyroscope sensor data. These graphs support the overall findings of the study, further confirming the absence of anomalies and the meaningfulness of the clustering results.

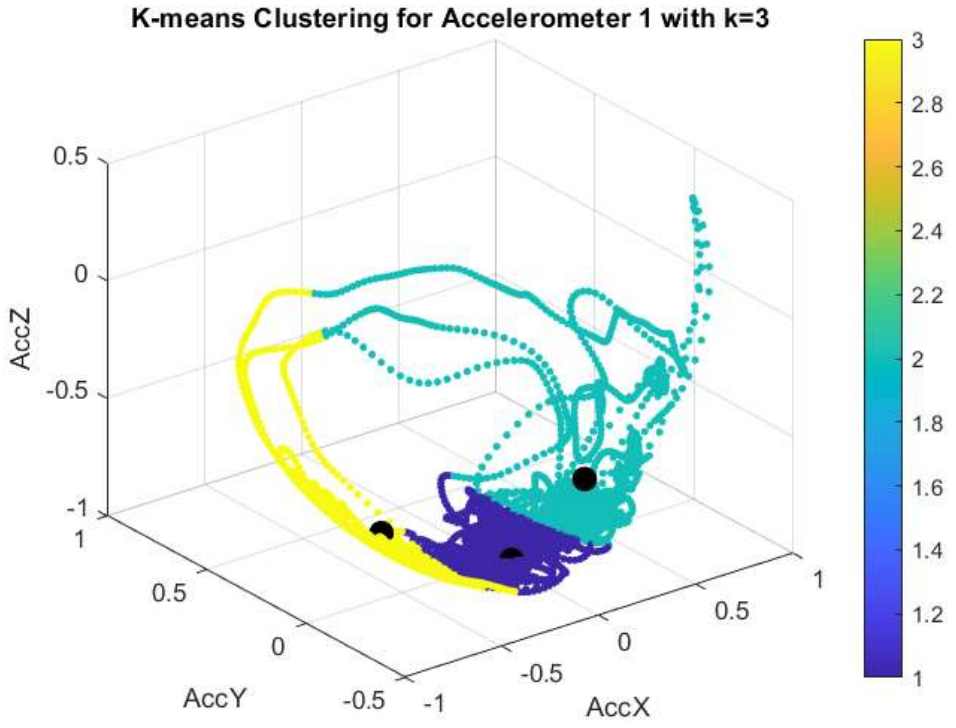

Fig. 26. Accelerometer 1 clustering result

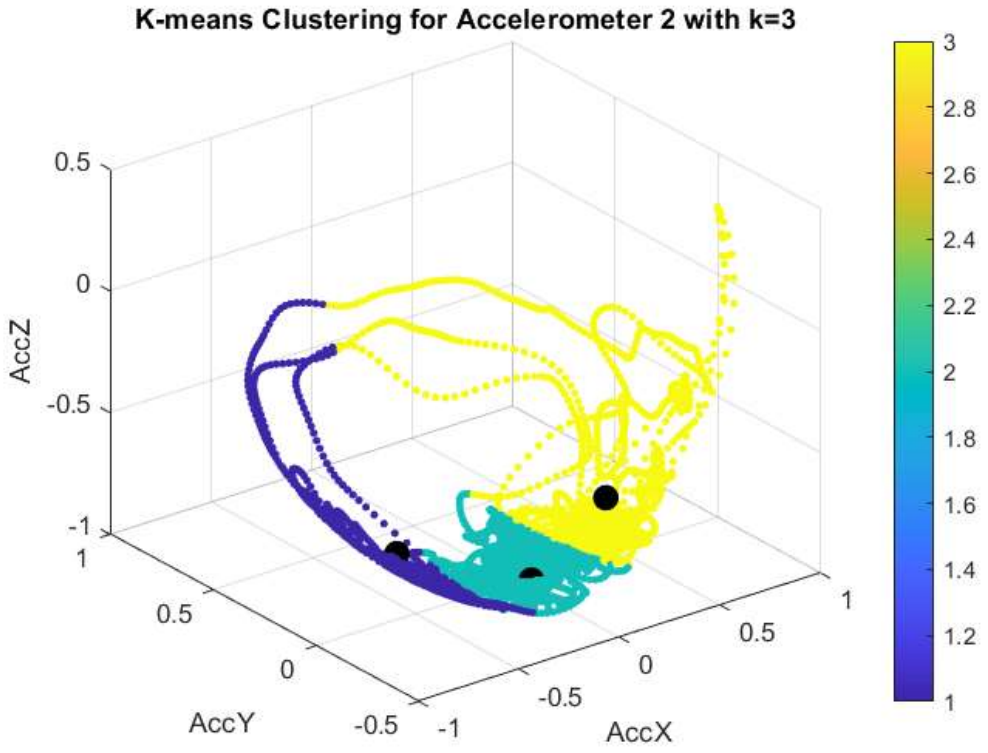

Fig. 27. Accelerometer 2 clustering result

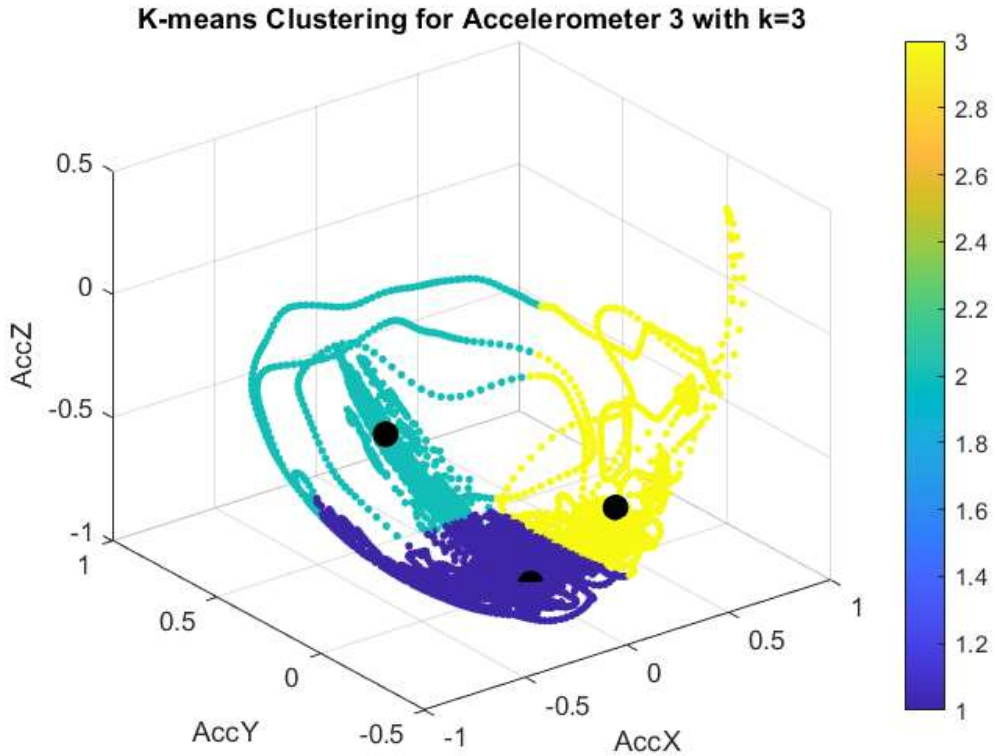

Fig. 28. Accelerometer 3 clustering result

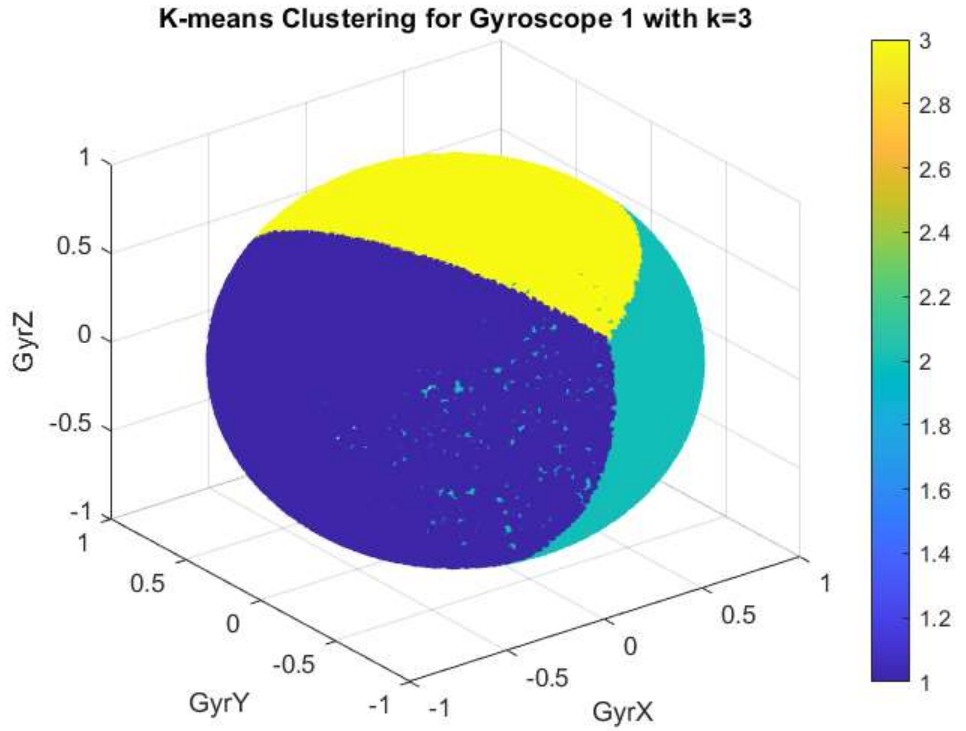

Fig. 29. Gyroscope 1 clustering result

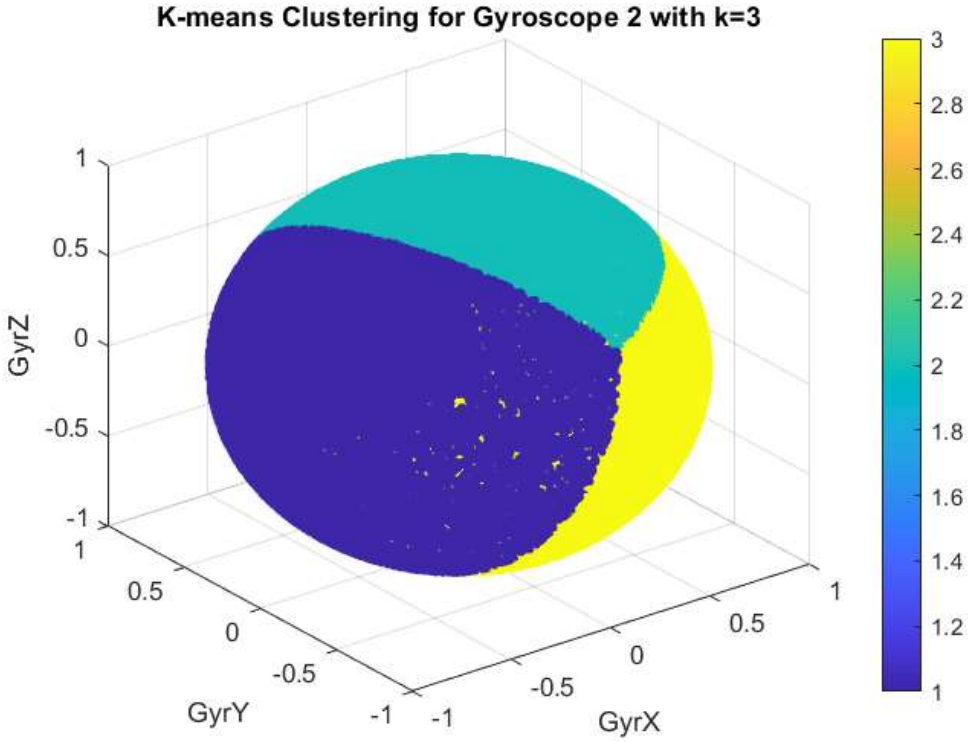

Fig. 30. Gyroscope 2 clustering result

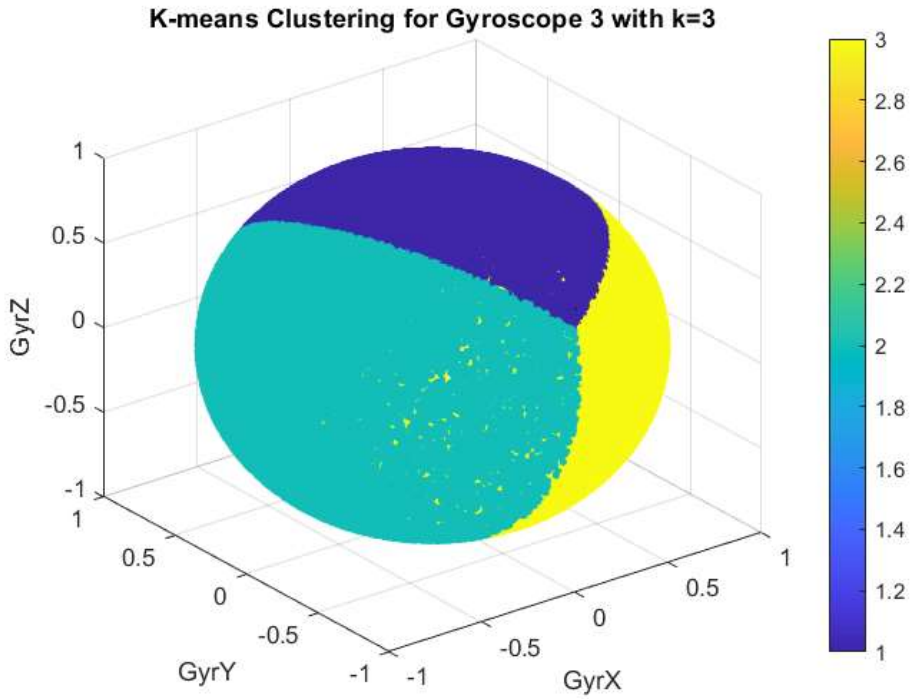

Fig. 31. Gyroscope 3 clustering result

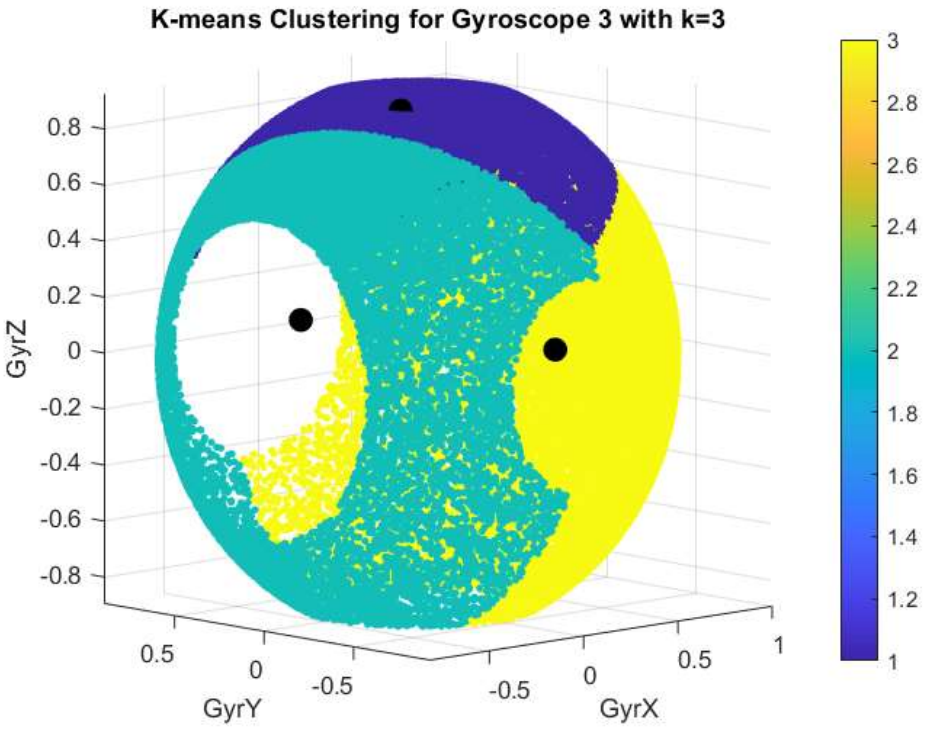

Fig. 32. Gyroscope 3 clustering result with centroid dot

The figures presented in this section (Figures 26, 27, 28, 29, 30, 31) depict the results of the clustering analysis. The centroids of the clustered datasets are represented by black dots. Additionally, Figure 32 illustrates the centroids of each clustered dataset using black dots. The colors in the figures indicate the specific clusters, with the corresponding values indicated in the accompanying color bar.

To understand why accelerometer and gyroscope clusters have different shapes requires appreciating their unique measurement abilities. Accelerometers are built specifically for measuring linear acceleration across different planes such as the X, Y, and Z ones. Therefore, any data they produce captures changes in acceleration which can appear scattered when represented across three-dimensional space. This randomness is a result of the varied acceleration patterns experienced by the vehicle during different phases of flight or operation.

In contrast, gyroscopes are utilized to measure angular velocity or rotational motion around different axes. Gyroscopes provide data on rotational rates, which, when plotted in a three-dimensional space, manifest as a spherical shape. This spherical representation arises from the continuous capture of rotational movements by the gyroscope sensors.

When analyzing clustering results related to integrated vehicle health management systems, it's essential to keep in mind certain factors that have an impact on how those results should be interpreted. These include elements such as the unique data context being examined, sensor characteristics involved in collection processes during testing or use scenarios for vehicles under consideration at different times or stages throughout their life-cycle development process - all which affect results interpretation thus making domain-specific knowledge key as well.

Conclusion of Results

The analysis of accelerometer and gyroscope readings in the context of integrated vehicle health management systems for autonomous aircraft and unmanned aerial vehicles has provided valuable insights. By employing spectrogram analysis and data processing techniques, we were able to identify variations in sensor performance across different operational scenarios. The processed data exhibited clear patterns and behaviors, improving the interpretability of the sensor data. Furthermore, clustering analysis revealed well-defined clusters without anomalies, indicating consistent characteristics within each cluster. These findings contribute to the understanding of data processing and clustering techniques in enhancing the analysis and interpretation of sensor data, paving the way for future research in this field.

Discussion

Additional analysis can be done by using machine learning algorithms to train the flight data and increase the accuracy of result comparisons. The primary focus of this study pertains to the examination of sensor-based IVHM systems for UAVs. Future research endeavors may involve the assessment of various parameters to further expand upon the findings presented here.

While this study provides valuable insights into the analysis of IVHM systems for UAVs, it is important to acknowledge that the obtained results were based solely on high-quality flight data. Therefore, it is highly recommended to complement these findings with an evaluation utilizing poor flight data in order to ascertain the robustness of the results.

Conclusion

In conclusion, this master's thesis was dedicated to a comprehensive analysis of Integrated Vehicle Health Management systems in unmanned aerial vehicles. The analysis focused specifically on accelerometer and gyroscope readings and their suitability for effective vehicle monitoring and maintenance practices. To facilitate data interpretation, a spectrogram technique was applied to examine the time-frequency characteristics of the sensor data, considering both raw and processed readings. The primary objective was to evaluate the impact of data processing techniques on the quality and reliability of the sensor data analysis.

The results derived from the spectrogram analysis yielded significant insights into the dynamic behavior and performance of UAVs. A comparison of the spectrograms between raw and processed data indicated that data processing techniques improved the readability and interpretability of the sensor data. The processed spectrograms revealed distinct patterns and behaviors, thereby facilitating an understanding of the vehicle's performance under various operational scenarios.

Furthermore, the study successfully identified specific flight states and behaviors, such as the commencement phase and the transition from autopilot to manual control. These findings were further validated through an external reference obtained from plot.ardupilot.org. Additionally, employing the silhouette score method for clustering analysis resulted in the successful grouping of similar data points into three well-defined clusters.

Within the accelerometer and gyroscope data, no anomalies were detected due to the nature of the sensor data. Graphical representations of the clustering results visually illustrated the absence of anomalies and offered insights into the distribution of data points within the clusters. The diverse shapes of the accelerometer and gyroscope clusters were attributed to their distinct measurement abilities, capturing changes in linear acceleration and rotational motion, respectively.

It is crucial to consider the contextual factors surrounding the analyzed data, including the specific characteristics of the sensors and the testing or operational scenarios of the vehicles. Domain-specific knowledge played a pivotal role in accurately interpreting the results.

Overall, this thesis significantly contributes to the understanding of integrated vehicle health management systems in UAVs and autonomous aircraft. The findings underscore the

effectiveness of data processing techniques in enhancing the analysis and interpretation of sensor data, thereby paving the way for further research and applications within this field.

References

Al-Hourani, A., Kandeepan, S., & Jamalipour, A. (2014). Modeling air-to-ground path loss for low altitude platforms in urban environments. 2014 IEEE Global Communications Conference, 2898–2904. https://doi.org/10.1109/GLOCOM.2014.7037248

An, D., Kim, N. H., & Choi, J. H. (2015, January). Practical options for selecting data-driven or physics-based prognostics algorithms with reviews. Reliability Engineering & System Safety, 133, 223–236.

Arslan, O. (2009). Design Of A Decision Support Architecture For Human Operators In Uav Fleet C2 Applications.

Benedettini, O., Baines, T. S., Lightfoot, H. W., & Greenough, R. M. (2009). State-of-the-art in integrated vehicle health management.

Cummings, M. L., Bruni, S., Mercier, S., & Mitchell, P. J. (2007). Automation Architecture for Single Operator, Multiple UAV Command and Control. www.dodccrp.org

Daponte, P., de Vito, L., Lamonaca, F., Picariello, F., Rapuano, S., & Riccio, M. (2017). Measurement science and education in the drone times. 2017 IEEE International Instrumentation and Measurement Technology Conference (I2MTC), 1–6. https://doi.org/10.1109/I2MTC.2017.7969979

David Reid (CNBC), Rolls-royce Is Developing Tiny ‘cockroach’ Robots to Crawl in and Fix Airplane Engines, CNBC, 2018 Available at: https://www.cnbc.com/ 2018/07/17/rolls-royce-is-developing-tiny-cockroach-robots-to-fix-airplaneengines.html , Accessed date: 25 March 2023.

Eswara, N., & Wanhill, P. R. J. H. (2017). Indian Institute of Metals Series Aerospace Materials and Material Technologies. http://www.springer.com/series/15453

Ezhilarasu, C. M., Skaf, Z., & Jennions, I. K. (2019, February). The application of reasoning to aerospace Integrated Vehicle Health Management (IVHM): Challenges and opportunities. Progress in Aerospace Sciences, 105, 60–73. https://doi.org/10.1016/j.paerosci.2019.01.001

Faisal, I. A., Purboyo, T. W., & Ansori, A. S. R. (2019). A Review of accelerometer sensor and gyroscope sensor in IMU sensors on motion capture. J. Eng. Appl. Sci, 15(3), 826-829.

Gao, S., Dai, X., Hang, Y., Guo, Y., & Ji, Q. (2018). Airborne Wireless Sensor Networks for Airplane Monitoring System. In Wireless Communications and Mobile Computing (Vol. 2018). Hindawi Limited. https://doi.org/10.1155/2018/6025825

Grahn, E. (2017). Evaluation of MEMS accelerometer and gyroscope for orientation tracking nutrunner functionality (Dissertation). Retrieved from http://urn.kb.se/resolve?urn=urn:nbn:se:kth:diva-215163

Hess, A., & Fila, L. (2002). Prognostics, from the need to reality – from the fleet users and PHM system designer/developers perspectives. In Proceedings of the 2002 IEEE Aerospace Conference, Montana, USA (pp. 2791-2797).

Hess, A., & Fila, L. (2002). The Joint Strike Fighter PHM concept: Potential impact on aging aircraft problems. In IEEE Aerospace Conference, Montana, USA (pp. 3021-3026).

Hess, A., Calvello, G., & Dabney, T. (2004). PHM a key enabler for the JSF autonomic logistics support concept. In IEEE Aerospace Conference, Montana, USA (pp. 3543-3550).

HU J, Y. J. J., & CAI W T. (2021). Analysis of integrated health management system for unmanned surface vehicle. https://doi.org/10.19693/j.issn.1673-3185

Jennions, I. K. (Ed.). (2013, September 30). Integrated Vehicle Health Management: The Technology.

Jin, Y., Minai, A. A., & Polycarpou, M. M. (2003). Cooperative real-time search and task allocation in UAV teams. 42nd IEEE International Conference on Decision and Control (IEEE Cat. No.03CH37475), 1, 7-12 Vol.1. https://doi.org/10.1109/CDC.2003.1272527

Johnson, S. B., Gormley, T., Kessler, S., Mott, C., Patterson-Hine, A., Reichard, K., Scandura, P. (2011). System Health Management.

John Wiley & Sons Lagkas, T., Argyriou, V., Bibi, S., & Sarigiannidis, P. (2018). UAV IoT Framework Views and Challenges: Towards Protecting Drones as "Things." Sensors, 18(11), 4015. https://doi.org/10.3390/s18114015

Luo, C., Nightingale, J., Asemota, E., & Grecos, C. (2015). A UAV-Cloud System for Disaster Sensing Applications. IEEE Vehicular Technology Conference, 2015. https://doi.org/10.1109/VTCSpring.2015.7145656

Marcy, H. O., Agre, J. R., Chien, C., Clare, L. P., Romanov, N., & Twarowski, A. (1999). Wireless Sensor Networks for Area Monitoring and Integrated Vehicle Health Management Applications. http://rsc.rockwell.com

Merwaday, A., & Guvenc, I. (2015). UAV assisted heterogeneous networks for public safety communications. 2015 IEEE Wireless Communications and Networking Conference Workshops, WCNCW 2015, 329–334. https://doi.org/10.1109/WCNCW.2015.7122576

Miguel Rasgado Baião, T., Calado Marta Alexandra Bento Moutinho, A., Fernando Alves da Silva Supervisor, J., & Bento Moutinho, A. (2017). Energy Monitoring System for Low-Cost UAVs Aerospace Engineering Examination Committee.

Mishra, M. K., Dubey, V., Mishra, P. M., & Khan, I. (2019). MEMS Technology: A Review. Journal of Engineering Research and Reports, 4(1), 1–24. https://doi.org/10.9734/jerr/2019/v4i116891

Motlagh, N. H., Bagaa, M., & Taleb, T. (2017). UAV-Based IoT Platform: A Crowd Surveillance Use Case. IEEE Communications Magazine, 55(2), 128–134. https://doi.org/10.1109/MCOM.2017.1600587CM

Mozaffari, M., Saad, W., Bennis, M., & Debbah, M. (2017). Mobile Unmanned Aerial Vehicles (UAVs) for Energy-Efficient Internet of Things Communications. IEEE Transactions on Wireless Communications, 16(11), 7574–7589. https://doi.org/10.1109/TWC.2017.2751045

Mozaffari, M., Saad, W., Bennis, M., Nam, Y.-H., & Debbah, M. (2019). A Tutorial on UAVs for Wireless Networks: Applications, Challenges, and Open Problems. IEEE Communications Surveys Tutorials, 21(3), 2334–2360. https://doi.org/10.1109/COMST.2019.2902862

Paixão de Medeiros, I., Ramos Rodrigues EMBRAER São José dos Campos, L. S., Santos, R., Hideiti Shiguemori, E., & Lúcio Nascimento Júnior, C. (2014). PHM-Based Multi-UAV Task Assignment.

Passaro, V. M. N., Cuccovillo, A., Vaiani, L., De Carlo, M., & Campanella, C. E. (2017). Gyroscope Technology and Applications: A Review in the Industrial Perspective. Sensors, 17(10), 2284. MDPI AG. Retrieved from http://dx.doi.org/10.3390/s17102284

PNGWing. (n.d.). Free PNG Image - PNGWing. accessed 2 April 2023. https://www.pngwing.com/en/free-png-smiqy/download

Prajapati , A. K., Roy, B. K., & Prasad, R. (2018, June 8). A State of Art Review of Integrated Vehicle Health Management System. IEEE. 2018 3rd International Conference for Convergence in Technology (I2CT), The Gateway Hotel, XION Complex, Wakad Road, Pune, India.

Ranasinghe, K., Sabatini, R., Gardi, A., Bijjahalli, S., Kapoor, R., Fahey, T., & Thangavel, K. (2022, January). Advances in Integrated System Health Management for mission-essential and safety-critical aerospace applications. Progress in Aerospace Sciences, 128, 100758. https://doi.org/10.1016/j.paerosci.2021.100758

Rodrigues, L., & Yoneyama, T. (2012). Spare parts inventory control for non-repairable items based on Prognostics and Health Monitoring information. Proceedings of the Annual Conference of the Prognostics and Health Management Society 2012, PHM 2012, 53–62.

Ruff, H., Calhoun, G., Draper, M., Fontejon, J., & Guilfoos, B. (2004). Exploring Automation Issues in Supervisory Control of Multiple UAVs. 7.

Saha, B., Koshimoto, E., Quach, C. C., Hogge, E. F., Strom, T. H., Hill, B. L., Vazquez, S. L., & Goebel, K. (2011). Battery health management system for electric UAVs. 2011 Aerospace Conference, 1–9. https://doi.org/10.1109/AERO.2011.5747587

Sanjiv Rao, G., & Vallikumari, V. (2012). A Beneficial Analysis Of Node Deployment Schemes For Wireless Sensor Networks. International Journal of Advanced Smart Sensor Network Systems, 2(2), 33–43. https://doi.org/10.5121/ijassn.2012.2204

Sarigiannidis, P., Lagkas, T., Bibi, S., Ampatzoglou, A., & Bellavista, P. (2017). Hybrid 5G optical-wireless SDN-based networks, challenges and open issues. IET Networks, 6(6), 141–148. https://doi.org/https://doi.org/10.1049/iet-net.2017.0069

Selany, S., Nasution, S. M., & Purboyo, T. W. (2015). Sosemanuk algorithm for encryption and decryption Video on Demand (VoD). In Proceedings of the 2015 IEEE Asia Pacific Conference on Wireless and Mobile (APWiMob'15) (pp. 125-129). IEEE.

Soorki, M. N., Mozaffari, M., Saad, W., Manshaei, M. H., & Saidi, H. (2016). Resource Allocation for Machine-to-Machine Communications with Unmanned Aerial Vehicles. 2016 IEEE Globecom Workshops (GC Wkshps), 1–6. https://doi.org/10.1109/GLOCOMW.2016.7849026

Turkrnani, A. M. D., & de Toledo, A. F. (1993). Modelling of radio transmissions into and within multistorey buildings at 900,1800 and 2300 MHz.

Unmanned Systems Technology. (2017). Battery Management Systems BMS & Battery Packs Overview.

Vachtsevanos, G., Lewis, F., Roemer, M., Hess, A., & Wu, B. (2006). Fault Diagnosis and Prognosis Performance Metrics. In Intelligent Fault Diagnosis and Prognosis for Engineering Systems (pp. 355–399). John Wiley & Sons, Ltd. https://doi.org/https://doi.org/10.1002/9780470117842.ch7

van Blyenburgh, P. (1999). UAVs: an overview. Air & Space Europe, 1(5), 43–47. https://doi.org/https://doi.org/10.1016/S1290-0958(00)88869-3

Walraven, Jeremy. (2003). Introduction to Applications and Industries for Microelectromechanical Systems (MEMS). 1. 674-680. 10.1109/TEST.2003.1270896.

Wang, D., Bai, L., Zhang, X., Guan, W., & Chen, C. (2012). Collaborative Relay Beamforming Strategies for Multiple Destinations with Guaranteed QoS in Wireless Machine-to-Machine Networks. International Journal of Distributed Sensor Networks, 8(8), 525640. https://doi.org/10.1155/2012/525640

Williams, Z. (2006). Benefits of IVHM: An analytical approach. In IEEE Aerospace conference, Big Sky, Montana, USA (pp. 4-11).

Woodard, S. E. (2003). Development and flight testing of an adaptable vehicle health-monitoring architecture. National Aeronautics and Space Administration, Langley Research Center.

Zanella, A., Bui, N., Castellani, A., Vangelista, L., & Zorzi, M. (2014). Internet of Things for Smart Cities. IEEE Internet of Things Journal, 1(1), 22–32. https://doi.org/10.1109/JIOT.2014.2306328

Zeng, Y., Zhang, R., & Lim, T. J. (2016). Wireless communications with unmanned aerial vehicles: opportunities and challenges. IEEE Communications Magazine, 54(5), 36–42. https://doi.org/10.1109/MCOM.2016.7470933

Zhu, K., & Pong, P. W. T. (2019). Curved Trapezoidal Magnetic Flux Concentrator Design for Current Measurement of Multi-Core Power Cable With Magnetic Sensing. IEEE Transactions on Magnetics, 55(4), 1–9. https://doi.org/10.1109/TMAG.2019.2893595

Zhu, K., Liu, X., & Pong, P. W. T. (2020). Performance study on commercial magnetic sensors for measuring current of unmanned aerial vehicles. IEEE Transactions on Instrumentation and Measurement, 69(4), 1397–1407. https://doi.org/10.1109/TIM.2019.2910339

ANNEXES

Codes used for analysis

1.1. MATLAB Code of Assigning k value

```
data = IMU;
AccData = data(:, 6:8);
AccData = unique(AccData, 'rows', 'stable');
AccData = AccData(~any(isnan(AccData), 2), :);
AccData = fillmissing(AccData, 'linear');
fc = 5; % Cutoff frequency (Hz)
fs = 100; % Sampling frequency (Hz)
[b,a] = butter(2, fc/(fs/2)); % 2nd-order Butterworth filter
AccData = filtfilt(b, a, AccData); % Zero-phase filtering
AccData_norm = AccData./sqrt(sum(AccData.^2, 2));
k_range = 2:10;
silhouette_scores = zeros(size(k_range));
for i = 1:length(k_range)
 k = k_range(i);
 idx = kmeans(AccData_norm, k);
 silhouette_scores(i) = mean(silhouette(AccData_norm, idx));
end
figure;
plot(k_range, silhouette_scores, '-o');
xlabel('Number of clusters (k)');
ylabel('Average silhouette score');
title('Silhouette method');
[best_score, best_k_idx] = max(silhouette_scores);
best_k = k_range(best_k_idx);
fprintf('Best k value: %d (average silhouette score = %.4f)\n', best_k,
 best_score);
```

2.2. Spectrogram MATLAB Code

```
data = IMU;
GyrData = data(:, 3:5); % Extract GyrX, GyrY, GyrZ
AccData = data(:, 6:8); % Extract AccX, AccY, AccZ
GyrData = unique(GyrData, 'rows', 'stable');
AccData = unique(AccData, 'rows', 'stable');
GyrData = GyrData(~any(isnan(GyrData), 2), :);
AccData = AccData(~any(isnan(AccData), 2), :);
AccData = fillmissing(AccData, 'linear');
GyrData = fillmissing(GyrData, 'spline');
fc = 5; % Cutoff frequency (Hz)
fs = 100; % Sampling frequency (Hz)
[b,a] = butter(2, fc/(fs/2)); % 2nd-order Butterworth filter
AccData = filtfilt(b, a, AccData); % Zero-phase filtering
GyrData = filtfilt(b, a, GyrData); % Zero-phase filtering
AccData_norm = AccData./sqrt(sum(AccData.^2, 2));
GyrData_norm = GyrData./sqrt(sum(GyrData.^2, 2));
mean_acc = mean(AccData_norm);
std_acc = std(AccData_norm);
corr_acc = corrcoef(AccData_norm);
mean_gyr = mean(GyrData_norm);
std_gyr = std(GyrData_norm);
corr_gyr = corrcoef(GyrData_norm);
N = size(GyrData_norm, 1); % Number of data points
f = (0:N/2)*(fs/N); % Frequency vector for FFT
GyrData_fft = fft(GyrData_norm);
GyrData_fft_mag = abs(GyrData_fft)/N; % Magnitude of the FFT
GyrData_fft_mag = GyrData_fft_mag(1:floor(N/2)+1, :); % Keep only the positive frequencies
window_size = 512;
noverlap = 256;
figure;
```

```
subplot(3,1,1)
spectrogram(GyrData_norm(:, 1), window_size, noverlap, [], fs, 'yaxis'); %
 Spectrogram for GyrX
subplot(3,1,2)
spectrogram(GyrData_norm(:, 2), window_size, noverlap, [], fs, 'yaxis'); %
 Spectrogram for GyrY
subplot(3,1,3)
spectrogram(GyrData_norm(:, 3), window_size, noverlap, [], fs, 'yaxis'); %
 Spectrogram for GyrZ
title(sprintf('Gyroscope Spectrogram'));
N = size(AccData_norm, 1); % Number of data points
f = (0:N/2)*(fs/N); % Frequency vector for FFT
AccData_fft = fft(AccData_norm);
AccData_fft_mag = abs(AccData_fft)/N; % Magnitude of the FFT
AccData_fft_mag = AccData_fft_mag(1:floor(N/2)+1, :); % Keep only the positive frequencies
window_size = 512;
noverlap = 256;
figure;
subplot(3,1,1)
spectrogram(AccData_norm(:, 1), window_size, noverlap, [], fs, 'yaxis'); % Spectrogram for AccX
subplot(3,1,2)
spectrogram(AccData_norm(:, 2), window_size, noverlap, [], fs, 'yaxis'); % Spectrogram for AccY
subplot(3,1,3)
spectrogram(AccData_norm(:, 3), window_size, noverlap, [], fs, 'yaxis'); % Spectrogram for AccZ
title(sprintf('Accelerometer Spectrogram'))
```

1.3. Clustering MATLAB Code

```
data = IMU;
GyrData = data(:, 3:5); % Extract GyrX, GyrY, GyrZ
AccData = data(:, 6:8); % Extract AccX, AccY, AccZ
GyrData = unique(GyrData, 'rows', 'stable');
AccData = unique(AccData, 'rows', 'stable');
GyrData = GyrData(~any(isnan(GyrData), 2), :);
AccData = AccData(~any(isnan(AccData), 2), :);
AccData = fillmissing(AccData, 'linear');
GyrData = fillmissing(GyrData, 'spline');
fc = 5; % Cutoff frequency (Hz)
fs = 100; % Sampling frequency (Hz)
[b,a] = butter(2, fc/(fs/2)); % 2nd-order Butterworth filter
AccData = filtfilt(b, a, AccData); % Zero-phase filtering
GyrData = filtfilt(b, a, GyrData); % Zero-phase filtering
AccData_norm = AccData./sqrt(sum(AccData.^2, 2));
GyrData_norm = GyrData./sqrt(sum(GyrData.^2, 2));
mean_acc = mean(AccData_norm);
std_acc = std(AccData_norm);
corr_acc = corrcoef(AccData_norm);
mean_gyr = mean(GyrData_norm);
std_gyr = std(GyrData_norm);
corr_gyr = corrcoef(GyrData_norm);
N = size(GyrData_norm, 1); % Number of data points
f = (0:N/2)*(fs/N); % Frequency vector for FFT
GyrData_fft = fft(GyrData_norm);
GyrData_fft_mag = abs(GyrData_fft)/N; % Magnitude of the FFT
GyrData_fft_mag = GyrData_fft_mag(1:floor(N/2)+1, :); % Keep only the positive frequencies
window_size = 512;
noverlap = 256;
figure;
```

```
subplot(3,1,1)
spectrogram(GyrData_norm(:, 1), window_size, noverlap, [], fs, 'yaxis'); % Spectrogram for GyrX
subplot(3,1,2)
spectrogram(GyrData_norm(:, 2), window_size, noverlap, [], fs, 'yaxis'); % Spectrogram for GyrY
subplot(3,1,3)
spectrogram(GyrData_norm(:, 3), window_size, noverlap, [], fs, 'yaxis'); % Spectrogram for GyrZ
title(sprintf('Gyroscope Spectrogram'));
N = size(AccData_norm, 1); % Number of data points
f = (0:N/2)*(fs/N); % Frequency vector for FFT
AccData_fft = fft(AccData_norm);
AccData_fft_mag = abs(AccData_fft)/N; % Magnitude of the FFT
AccData_fft_mag = AccData_fft_mag(1:floor(N/2)+1, :); % Keep only the positive
 frequencies
window_size = 512;
noverlap = 256;
figure;
subplot(3,1,1)
spectrogram(AccData_norm(:, 1), window_size, noverlap, [], fs, 'yaxis'); %
 Spectrogram for AccX
subplot(3,1,2)
spectrogram(AccData_norm(:, 2), window_size, noverlap, [], fs, 'yaxis'); %
 Spectrogram for AccY
subplot(3,1,3)
spectrogram(AccData_norm(:, 3), window_size, noverlap, [], fs, 'yaxis'); %
 Spectrogram for AccZ
title(sprintf('Accelerometer Spectrogram'))
```